

The Plant Journal (2025) 123, e70356

doi: 10.1111/tpj.70356

# Barley resistance and susceptibility to fungal cell entry involve the interplay of ROP signaling with phosphatidylinositol-monophosphates

Lukas Sebastian Weiß<sup>1</sup>, Mariem Bradai<sup>1</sup>, Christoph Bartram<sup>1</sup>, Mareike Heilmann<sup>2</sup>, Julia Mergner<sup>3,4</sup>, Bernhard Kuster<sup>3,4</sup>, Götz Hensel<sup>5,6</sup>, Jochen Kumlehn<sup>5</sup>, Stefan Engelhardt<sup>1</sup>, Ingo Heilmann<sup>2</sup>, and Ralph Hückelhoven<sup>1,\*</sup>

Received 2 January 2025; revised 2 July 2025; accepted 7 July 2025. \*For correspondence (e-mail hueckelhoven@tum.de).

#### **SUMMARY**

Rho-of-plant small GTPases (ROPs) are regulators of plant polar growth and of plant-pathogen interactions. The barley ROP, RACB, is involved in susceptibility toward infection by the barley powdery mildew fungus Blumeria hordei (Bh) but little is known about the cellular pathways that connect RACB signaling to disease susceptibility. Here we identify novel RACB interaction partners of plant or fungal origin by untargeted co-immunoprecipitation of constitutively active (CA) RACB tagged by green fluorescent protein from Bhinfected barley epidermal layers and subsequent analysis by liquid chromatography-coupled mass spectrometry. Three of the immunoprecipitated proteins, a plant phosphoinositide phosphatase, a plant phosphoinositide phospholipase, and a putative Bh-effector protein, are involved in the barley-Bh-pathosystem and support disease resistance or susceptibility, respectively. RACB and its plant interactors bind to overlapping anionic phospholipid species in vitro, and in the case of RACB, this lipid interaction is mediated by its carboxy-terminal polybasic region (PBR). Fluorescent markers for anionic phospholipids show altered subcellular distribution in barley cells during Bh attack and under expression of a RACB-binding fungal effector. Phosphatidylinositol 4-phosphate, phosphatidylinositol 3,5-bisphosphate, and phosphatidylserine show a distinct enrichment at the haustorial neck region, suggesting a connection to subcellular targeting of RACB at this site. The interplay of ROPs with anionic phospholipids and phospholipid-metabolizing enzymes may thus enable the subcellular enrichment of components pivotal for success or failure of fungal penetration.

Keywords: effector, haustorium, phosphatidylinositol-monophosphate, phosphoinositide phosphatase, phosphoinositide phospholipase, polarity, polybasic domain, ROP GTPAse, susceptibility.

#### INTRODUCTION

Although plant immunity is increasingly well understood, the understanding of mechanisms of disease susceptibility is still far from complete. Pathogen effectors target host proteins for suppression of plant immunity or trigger the function of plant negative regulators of immunity. Beyond this, some host susceptibility factors do not act in regulation of host immunity but serve the pathogens' demands in nutrition or in transforming host cell architecture (Saur & Hückelhoven, 2021; van Schie & Takken, 2014). Specific

Rho-of-plant small monomeric GTPases (ROPs) might function as such susceptibility factors (Schultheiss et al., 2003). ROPs are the only representatives of the Rho-family of small GTPases that are found in plants (Yang, 2002), and historically have also been termed RACs (rat sarcoma-related C botulinum substrate) (Winge et al., 2000). ROPs are considered as regulators of polar signaling processes in development, but can also regulate stress and immune responses (Akamatsu et al., 2013; Fratini et al., 2021; Jones et al., 2002; Kost et al., 1999). ROP

<sup>&</sup>lt;sup>1</sup>Chair of Phytopathology, TUM School of Life Sciences, Technical University of Munich, Freising, Germany,

<sup>&</sup>lt;sup>2</sup>Department of Plant Biochemistry, Institute of Biochemistry and Biotechnology, Martin-Luther-University Halle-Wittenberg, Halle (Saale), Germany,

<sup>&</sup>lt;sup>3</sup>Chair of Proteomics and Bioanalytics, Technical University of Munich, Freising, Germany,

<sup>&</sup>lt;sup>4</sup>Bavarian Biomolecular Mass Spectrometry Center (BayBioMS), Technical University of Munich, Freising, Germany,

<sup>&</sup>lt;sup>5</sup>Institute of Plant Genetics and Crop Plant Research, Gatersleben, Germany, and

<sup>&</sup>lt;sup>6</sup>Heinrich Heine University Düsseldorf, Faculty of Mathematics and Natural Sciences, Centre for Plant Genome Engineering, Düsseldorf, Germany

signaling depends on the binding of ROPs to guanine nucleotides, and ROPs bound to GDP are signalinginactive, whereas GTP-bound ROPs are competent (Berken, 2006). In some cases, the interaction between ROPs and downstream signaling proteins (here called executors) can be indirect and may require the presence of scaffolding proteins. Interactors of constitutive active ROPs (ICRs; also called ROP-interactive partners (RIPs)) and ROP-interactive and CRIB-motif containing proteins (RICs) have previously been described as relevant ROP scaffolds (Engelhardt et al., 2023; Lavy et al., 2007; Li et al., 2008; McCollum et al., 2020; Wu et al., 2001). In Arabidopsis thaliana (At), RICs mediate ROP-effects on cytoskeletal organization, pavement cell morphogenesis or hormone responses (Choi et al., 2013; Fu et al., 2009; Gu et al., 2005; Lin et al., 2013; Wu et al., 2001; Zhou et al., 2015). Activated ROPs associate with the plasma membrane through C-terminal sequence motifs in the hypervariable region of the ROP proteins. In particular, a polybasic region (PBR) of positively charged lysine and arginine residues has been proposed to be essential for the interaction with membrane lipids in vitro, and for the recruitment of ROPs into anionic phospholipid-containing plasma membrane domains in planta (Platre et al., 2019; for fundamental work compare also Heo et al., 2006). For PM-interaction, type I ROPs are additionally cysteine-prenylated at the carboxyterminal CaaX-box motif and can be additionally and reversibly S-acylated (Sorek et al., 2017). Type II ROPs are constitutively S-acylated at their GC-CG-box (Yalovsky, 2015).

The membrane positioning of ROPs has been proposed to be governed in part by the presence of anionic phospholipids (Platre et al., 2019; Sternberg et al., 2021). Anionic phospholipid species constitute less than 1% of all lipids in plant leaves, but play vital roles in plant development and polar growth processes (Noack & Jaillais, 2020). Phosphoinositides (Ptdlns) are an important group of anionic phospholipids that are formed by the phosphorylation of the membrane lipid phosphatidylinositol by specific lipid kinases at specific hydroxyl groups of the inositol head group. Reversely, PtdIns can be dephosphorylated by specific phosphatases or the inositol-phosphate headgroup can be cleaved from the diacylglycerol backbone by phospholipases (Gerth et al., 2017; Mueller-Roeber & Pical, 2002; Zhong & Ye, 2003). Another anionic phospholipid, phosphatidylserine (PtdSer), is generated by the addition of L-serine to phosphorylated diacylglycerol or via headgroup exchange from phosphatidylcholine or phosphatidylethanolamine with L-serine. With the help of genetically encoded cellular lipid markers and reverse genetics, a role for anionic phospholipids in stress responses, cellular trafficking processes, and cell polarity was established (Gerth et al., 2017; Noack & Jaillais, 2020; Qin et al., 2020; van Leeuwen et al., 2007). Importantly, anionic phospholipids serve as targeting signals for proteins such as ROPs and their interactors (Kulich et al., 2020; Platre et al., 2019), and both PtdIns and PtdSer have been shown to influence the distribution of ROPs at plant membranes (Fratini et al., 2021; Platre et al., 2019). For instance, PtdSer-dependent recruitment of AtROP6 through its PBR is essential for ROP-dependent downstream processes during root gravitropism (Platre et al., 2019). Type II ROPs, too, require an intact PBR for lipid interaction and positioning in plasma membrane domains (Lavy & Yalovsky, 2006; Sternberg et al., 2021).

A possible interplay of ROPs with anionic phospholipids during plant-pathogen interactions is less well established. The barley ROP, RACB, acts in signaling processes supporting susceptibility toward infection by the barley powdery mildew fungus Blumeria hordei (Bh) (Hoefle et al., 2011; Schultheiss et al., 2002; Schultheiss et al., 2003). Overexpression of constitutively activated RACB (RACB-CA) leads to more frequent fungal cell entry and formation of haustoria in intact plant cells that engulf the apoplastic fungal infection structure with an extrahaustorial matrix and an extrahaustorial membrane of host origin. Gene silencing of RACB limits Bh's penetration success and haustorial expansion, highlighting the role of RACB as a susceptibility factor (Hoefle et al., 2011, Schultheiss et al., 2002, Schultheiss et al., 2003). Interestingly, the signaling-active form of RACB appears to be required for its role as a susceptibility factor, as only overexpression of RACB-CA enhanced fungal infection success, whereas neither the overexpression of wild-type (WT) RACB nor the dominant negative (DN) RACB increased barley susceptibility (Schultheiss et al., 2003). Several RACB-interacting executors and regulators are also involved in the barley-Bh pathosystem (Hoefle et al., 2011; Huesmann et al., 2012; Reiner et al., 2016; Trutzenberg et al., 2022) and three RACB-binding scaffold proteins, RIC157, RIC171, and RIPb, can support susceptibility toward Bh when overexpressed. Furthermore, RIC157, RIC171, and RIPb interact with activated RACB at the PM in planta. During Bh attack, these ROP scaffolds localize to the haustorial neck region together with RACB (Engelhardt et al., 2023; McCollum et al., 2020; Schultheiss et al., 2008). PM localization of RACB appears to be essential for its role in susceptibility, since a truncated RACB mutant that lacks the prenylation motif "CSIL" mislocalizes to the cytosol and does not enhance fungal penetration (Schultheiss et al., 2003; Weiss et al., 2022). While the role of RACB as a susceptibility factor in the barley-Bh pathosystem is well supported, it remains unclear how RACB is subcellularly positioned and how the RACB signaling machinery may be recruited to the site of fungal entry at the PM.

Here, we identify three RACB interaction partners of plant and fungal origin, which establish a link between RACB and anionic phospholipids known to serve as

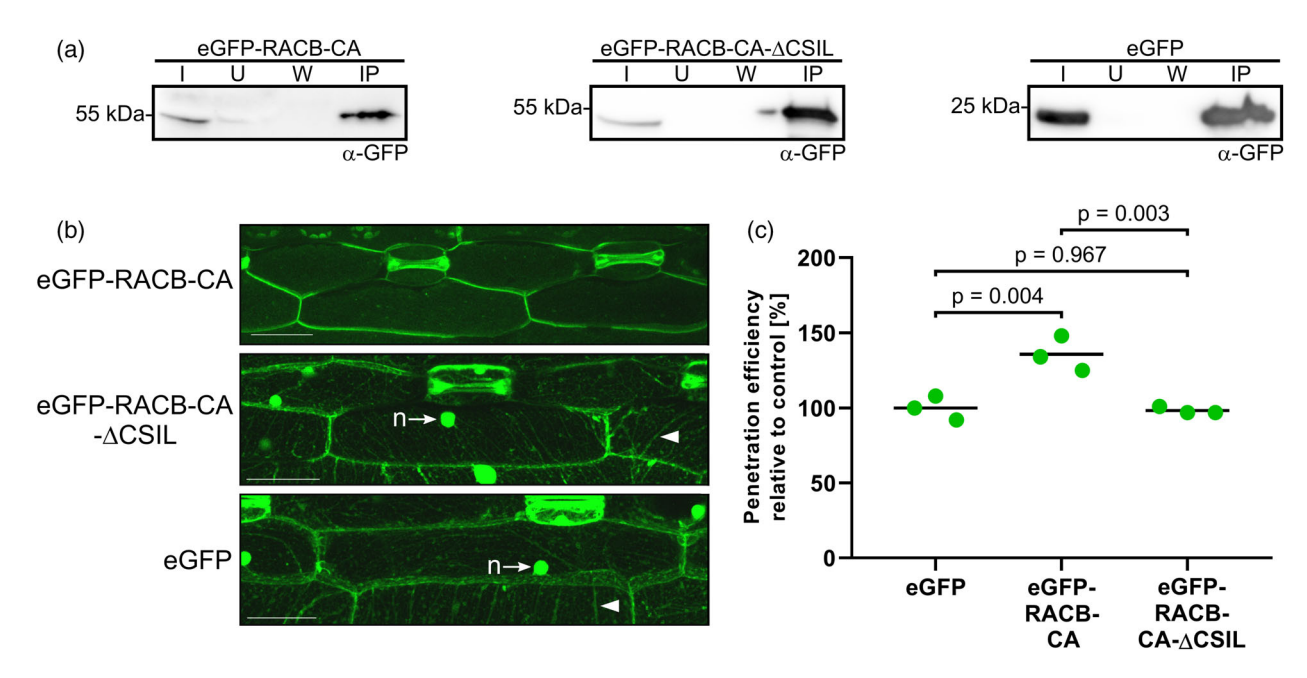


Figure 1. Transgenic barley plants overexpressing plasma membrane-localized eGFP-RACB-CA are super-susceptible to Bh infection. (a) eGFP and tagged fusion proteins show stable expression in first barley leaves and can be enriched via α-GFP IP. eGFP-tagged proteins were detected by α-GFP Western blotting, IP fractions; Input (I), Unbound (U), Wash (W) and enriched proteins (IP)

(b) Full-length eGFP-RACB-CA localizes to the PM of barley epidermal cells, while eGFP-RACB-CA-∆CSIL and free eGFP are visible in the cytosol (arrowhead: cytosolic strands) and nucleus (n, arrows). CLSM investigated subcellular localization. Scale bar: 50 µm. Images are maximum projections of at least 29 Z-steps of 2 µm increment optical sections. Image brightness was uniformly enhanced post-scanning for better visibility.

(c) Overexpression of full-length eGFP-RACB-CA renders barley plants more susceptible to Bh invasion, whereas eGFP-RACB-CA-∆CSIL and free eGFP show similar levels of lower susceptibility. For each construct, three primary leaves of one plant line were tested. Lines were: BG654 E2 for eGFP-RACB-CA, BG655 E1 for eGFP-RACB-CA-\(\Delta\)CSIL and BG656 E1 for eGFP. Each data point represents the susceptibility of one leaf that was analyzed at 100 interaction sites. Crossbar depicts average susceptibility relative to the eGFP control. Statistical analysis was performed using a one-way ANOVA with Tukey's honestly significant difference test.

position signals for protein-PM-recruitment. Anionic phospholipid markers display a distinct pattern of subcellular distribution during Bh attack, indicating a potential function in the barley-Bh-pathosystem. The identified RACB-interacting proteins as well as RACB all bind anionic phospholipids in vitro. RACB, binding to anionic phospholipids requires its intact PBR, and a RACB PBR substitution variant, RACB-5Q, defective in lipid binding in vitro, fails to localize to the PM in planta and is no longer signaling-competent with regard to barley susceptibility toward Bh. Together, the data indicate functional interplay between RACB and anionic phospholipids during barley/Bh interactions.

#### **RESULTS**

## PM localization is essential for RACB's role as a susceptibility factor

To enable protein co-immunoprecipitation (Co-IP) studies with tagged RACB, we generated stable transgenic barley lines overexpressing enhanced green fluorescent protein (eGFP)-tagged CA RACB, eGFP-RACB-CA, a RACB substitution variant lacking the four terminal amino acids "CSIL" of the CaaX-box prenylation site (eGFP-RACB-CA-ΔCSIL),

or expressing free eGFP as control. We initially obtained 27 transformation events overexpressing eGFP-RACB-CA, 14 events for eGFP-RACB-CA- $\Delta$ CSIL and 17 for eGFP. After propagation of these independent events, offspring with the correct genotypes were identified by PCR, Western blotting, and resistance against the selection marker hygromycin. Two independent transgenic lines for each construct were used for subsequent experiments. Using  $\alpha$ -GFP Western blotting, we found that all fusion proteins were expressed in full size and could be enriched via α-GFP immunoprecipitation (IP; see Figure 1a). The full-length eGFP-RACB-CA fusion localized to the PM of barley epidermal cells when analyzed by confocal laser scanning microscopy (CLSM). In contrast, the truncated eGFP-RACB-CA-ΔCSIL variant proved expectedly in the cytosol and the nucleus, similar to free eGFP (see Figure 1b). Moreover, plants overexpressing full-length eGFP-RACB-CA were more susceptible to haustorial invasion by Bh when compared with plants overexpressing eGFP-RACB-CA-∆CSIL or free eGFP (see Figure 1c). This showed that the full-length eGFP-RACB-CA fusion expressed in the transgenic barley lines was functional as a susceptibility factor. The observation that eGFP-RACB-CA-∆CSIL did not mediate enhanced susceptibility is consistent with earlier findings that 4 of 20 Lukas Sebastian Weiß et al.

RACB-CA needs to be PM-localized to act (Schultheiss et al., 2003; Weiss et al., 2022).

# Co-immunoprecipitation identifies novel RACB-CA interactors

To identify novel RACB protein interaction partners, we performed an untargeted Co-IP from transgenic eGFP-RACB-CA plants. eGFP-tagged proteins and associated putative interaction partners were co-immunoprecipitated at 24 h post-inoculation (hpi) from Bh-infected (or mocktreated) epidermal peels from first leaves of transgenic proteins were identified barley, by chromatography-coupled tandem mass spectrometry (LC-MS/MS; see Figure S1). We used epidermal peels for this screening, because Bh only colonizes the epidermal cell layer of barley. Overall, we detected 1399 unique proteins of plant and fungal origin in the LC-MS/MS analysis that were ranked according to statistically significant enrichment in eGFP-RACB-CA samples and the presence of unique peptides. Comparison of Bh-infected full-length eGFP-RACB-CA and free eGFP samples revealed 24 proteins that were significantly enriched with eGFP-RACB-CA (full dataset in Table \$1). Under mock-inoculation conditions, 17 proteins were significantly enriched in samples from eGFP-RACB-CA-expressing plants. In the infected samples, one protein of Bh origin stood out, as it was more than 60-fold enriched and found in all biological and technical replicates of each eGFP-RACB-CA and eGFP-RACB-CA-ΔCSIL and was annotated as a putative Bheffector protein (N1JEY6 BLUG1). We called this protein 909 for "found in 9 out of 9 replicates." Among identified proteins of plant origin, we focused on two new possible interaction partners after comparing the curated dataset with literature data, because these proteins were annotated in the context of phospholipid metabolism. During mock conditions, a phosphoinositide phospholipase C-like protein was significantly enriched with eGFP-RACB-CA (Student's t-test P < 0.01), whereas during infection a PtdIns phosphatase was exclusively enriched in samples from eGFP-RACB-CA-expressing plants (P < 0.001). detailed analysis of the corresponding proteins identified their nature as Hordeum vulgare phospholipase C1 (HvPLC1, HORVU2Hr1G013730.2) and suppressor of actin (SAC) phosphoinositide phosphatase HvSAC-like (HOR-VU4Hr1G077220.4) (Figures S2 and S3). The 9o9 protein shares a phylogenetic origin with classical Bh candidate secreted effector proteins (CSEPs) (Pedersen et al., 2012; Spanu et al., 2010), while it lacks a clearly predicted secretion signal.

# In vivo interaction between RACB and 909, PLC1 and SAC-like

To test whether the immunoprecipitated 909, PLC1, and SAC-like proteins are direct interaction partners of barley

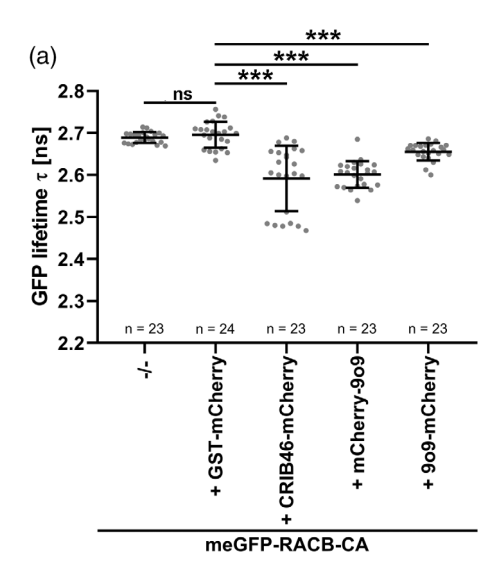
RACB, we investigated their ability to interact in targeted assays. For Förster-Resonance Energy Transfer Fluorescence Lifetime Imaging Microscopy (FRET-FLIM) in Nicotiana benthamiana, we expressed monomeric eGFP (meGFP) fused to the N-terminus of RACB-CA as a FRET donor, and co-expressed N- or C-terminal mCherry fusions of 909, PLC1, and SAC-like as FRET acceptors. C-terminally mCherry-tagged glutathione S-transferase (Kulich et al.) and CRIB46, a ROP GTPase-interactive protein domain of the RACB-CA interaction partner RIC171 (Schultheiss et al., 2008; Trutzenberg et al., 2022), were used as negative and positive controls, respectively. In the FRET-FLIM analyses, both mCherry fusions of 909 decreased the GFP lifetime of meGFP-RACB-CA, indicative of direct proteinprotein interaction (Figure 2a). C-terminally tagged PLC1mCherry and N-terminally tagged mCherry-SAC-like also reduced the lifetime of meGFP-RACB-CA (Figure 2b,c). The FRET-FLIM analyses indicate that 909 from Bh, and PLC1 and the SAC-like protein from barley can directly interact with RACB-CA in planta. While fusions of 909 to both Cterminal or N-terminal mCherry tags resulted in significantly reduced fluorescence lifetime of meGFP-RACB-CA, data for PLC1 or SAC-like were only significant for the Cterminal or N-terminal mCherry fusion of PLC1 or SAC-like, respectively (Figure 2b,c). These differences might result from protein-specific features of the fluorescence fusions and possibly indicate a weaker interaction of PLC1 or SAClike with RACB-CA.

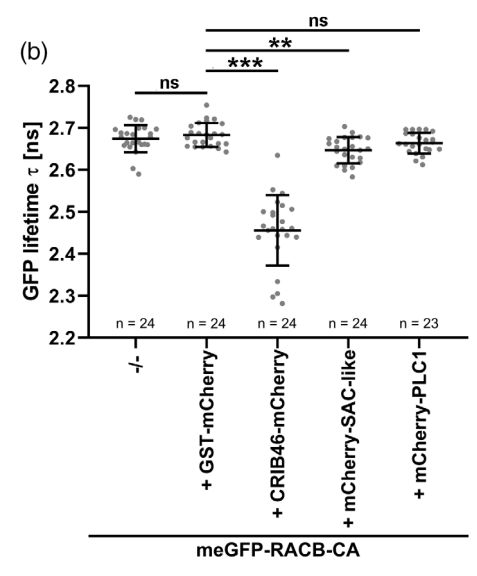
#### 909 Expression increases during Bh infection

To further characterize the three candidate RACB interactors in the context of Bh infection of barley plants, we investigated their expression by RT-qPCR (Figure 3). A publicly available barley RNAseq dataset (Mascher et al., 2017; Rapazote-Flores et al., 2019) identified transcripts of PLC1 and SAC-like in several barley tissues. Since both genes showed moderate expression levels in the epidermal cell layer that is colonized during fungal invasion, we analyzed whether 909, PLC1, or SAC-like were differentially expressed in epidermal cells upon Bh attack. Transcript abundance of PLC1, SAC-like, and 909 was assessed in the barley epidermis at 6, 12, and 24 h after Bh inoculation (Figure 3). The 909 transcript increased over time, up to approx. 100-fold at 24 hpi compared with its initial transcript levels in spores and normalized to fungal tubulin gene expression (Figure 3a). By contrast, the transcript abundance for the two plant genes did not strongly change upon Bh infection (Figure 3b,c).

# PLC1, SAC-like and 909 influence the barley-Bh interaction

The data indicated that the RACB interactors, PLC1 and SAC-like, are expressed in barley tissues that are colonized by *Bh* and showed an upregulation of the *Bh* effector 909 during the infection process. To test a possible role of the





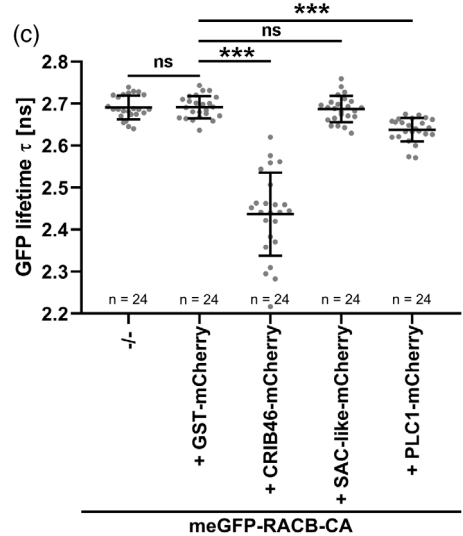


Figure 2. RACB-CA interacts with 909, PLC1, and SAC-like in FRET-FLIM experiments

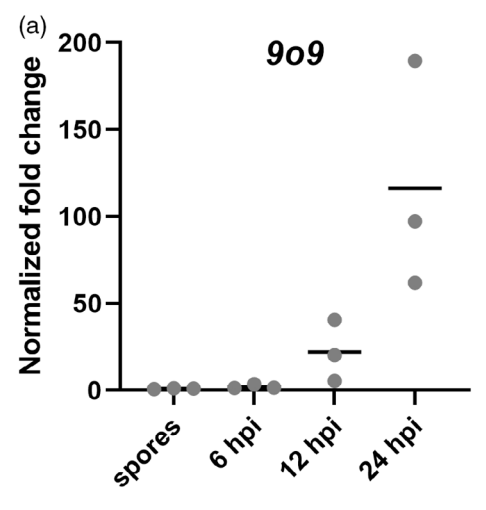
- (a) Co-expression of N- or C-terminally mCherry-tagged 9o9 decreased the fluorescence lifetime of GFP-RACB-CA, which indicates direct proteinprotein interaction
- (b) N-terminally tagged mCherry-SAC-like but not mCherry-PLC1 significantly reduced the fluorescence lifetime of GFP-RACB-CA.
- (c) C-terminally tagged PLC1-mCherry but not SAC-like-mCherry decreased the lifetime of GFP-RACB-CA. GST-mCherry and CRIB46-mCherry were used as negative and positive controls, respectively (Schultheiss et al., 2008; Trutzenberg et al., 2022). FRET-FLIM measurements were conducted at the cell periphery of epidermal cells of transiently transformed Nicotiana benthamiana plants. Co-expression of fusion proteins was confirmed before measurements. All measurements were collected in three independent biological replicates. The number of observations (n) per construct is shown below each column. The crossbar and error bars show the average and standard deviation. Statistical differences were calculated with Wilcoxon-Rank-Sum tests with Bonferroni correction. ns P > 0.05, \*\*P < 0.01, \*\*\*P < 0.001. -/-: FRFT-donor-only control.

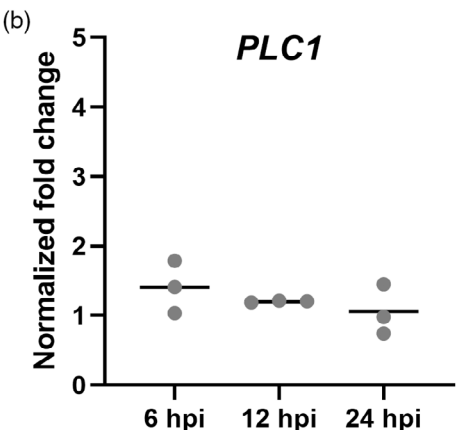
RACB interactors in the barley-Bh interaction, we transiently expressed these proteins in barley plants under the control of the cauliflower mosaic virus 35S promoter, or we silenced expression using RNA interference (RNAi) before plants were inoculated with Bh. Overexpression of 909 in barley epidermal cells increased the relative barley susceptibility toward Bh invasion on average by 36% over the susceptibility of empty vector controls, as determined by counting haustoria frequencies at 40 hpi in individual transformed cells that were attacked by Bh. By contrast, RNAi (host-induced gene silencing) against 909 did not influence the penetration efficiency of Bh (Figure 4a,b). Conversely, RNAi against PLC1 or SAC-like increased barley susceptibility toward Bh infection on average by 36% or 67%, respectively, compared with empty vector controls (Figure 4c,d), whereas overexpression of PLC1 or SAC-like did not change the susceptibility of barley against Bh. Data indicate that 909, PLC1, and SAC-like have opposing roles in the barley-Bh interaction, with ectopic fungal 909 expression promoting susceptibility and barley PLC1 and SAC-like limiting fungal penetration success.

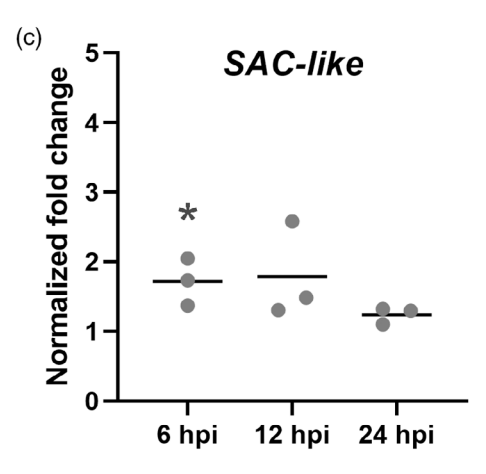
## RACB, PLC1, and SAC-like show overlapping patterns of lipid-binding capabilities

The requirement of PM association of RACB (cf. Figure 1) as well as the interaction of RACB with PLC1 or SAC-like proteins (cf. Figure 2) suggested a link between RACB function and anionic phospholipids. Like other ROPs (Platre et al., 2019), RACB contains a PBR predicted to bind anionic phospholipids. Computational analysis suggested that PLC1 and SAC- like proteins can also interact with phospholipids and potentially possess enzymatic activity against phosphoinositides. To investigate which phospholipids might bind to the 909, PLC1 or SCA-like proteins, in vitro lipid-binding assays were performed with recombinantly expressed GST- or Myelin Basic Protein (MBP)-tagged

and-conditions) on Wiley Online Library for rules of use; OA articles are governed by the applicable Creative Commons Licenso







proteins (Figure 5). A GST-tagged RACB-WT protein was included in these experiments that is similar to *Arabidopsis thaliana At*ROP6, which has previously been shown to display lipid-binding capacity (Platre et al., 2019). In protein-lipid-overlay experiments, GST-RACB-WT and its MBP-tagged PLC1 and SAC-like interactors displayed similar lipid-binding features and bound to PtdIns-

Figure 3. Gene expression of Bh 909 increases during Bh invasion.

The expression levels of Bh 909 (a) and barley PLC1 (b) and SAC-like (c) were measured during the early phase of Bh colonization at the indicated timepoints. Transcript of 909 was detectable in spores and increased during infection. Expression levels of PLC1 and SAC-like only slightly differed during infection but showed partially significant differences compared with their non-infected controls (as indicated by the P-values). Bars show reference gene-normalized fold changes in infected leaves, which were calculated according to using normalized gene expression in spores (a) or corresponding non-infected leaves (b, c) as a baseline. β-TUB2 was chosen as a reference gene for Bh. while UBC2 was taken as housekeeping genes for barley (Schnepf et al., 2018; Sherwood & Somerville, 1990). Bars show average fold changes in normalized gene expression with standard deviation. Data was collected over three independent biological replicates. Statistical differences were calculated separately for each timepoint and gene, comparing the normalized expression of PLC1 and SAC-like in infected leaves to that of corresponding non-infected leaves. Differences were assessed using t-tests with Holm-Sidak correction for multiple testing and only indicated in the graph when significant, \*P < 0.05.

monophosphates (PtdIns3P, PtdIns4P and PtdIns5P) (Figure 5). In a GST-RACB-5Q substitution variant (RACB-K184Q, K185Q, K186Q, K187Q, K188Q), the substitution of five lysine residues in the PBR for uncharged glutamine (Q) residues fully abolished lipid binding (Figure 5).

# RACB's PBR is essential for its signaling function and membrane localization

Since the RACB-5Q substitution variant did not bind phospholipids, we investigated whether PBR mutants were functional in planta. As the PBR of the related AtROP6 has previously been shown to mediate membrane association of AtROP6 (Platre et al., 2019), we first compared the subcellular localization of a GFP-RACB-5Q fusion with that of GFP-RACB-CA in barley epidermal cells. We further investigated whether the RACB-CA-5Q variant still interacted with its downstream partner, the canonical RACB interactor and ROP scaffold, RIC171. Using CLSM of transiently transformed barley epidermal cells (Figure 6), soluble CFP, GFP, and mCherry-RIC171 fusions, expressed as controls, displayed cytoplasmic and nucleoplasmic fluorescence distributions (Figure 6a, top panels). By contrast, when GFP-RACB-CA was co-expressed instead of the GFP control, both GFP-RACB-CA and mCherry-RIC171 signals were detected at the PM and for mCherry-RIC171 additionally in the nucleus (Figure 6a, mid-panels). The data are consistent with the previous report that PM-associated RACB-CA can recruit RIC171 to the cell periphery (Schultheiss et al., 2008; Trutzenberg et al., 2022). By contrast, GFP-RACB-CA-5Q mislocalized to the cytoplasm and nucleoplasm (Figure 6a, bottom panel). Moreover, in cells co-expressing GFP-RACB-CA-5Q and mCherry-RIC171, mCherry-RIC171 was not detected at the cell periphery but remained in the cytoplasm and nucleoplasm (Figure 6a, bottom panels) in a similar distribution as was observed upon co-expression of mCherry-Ric171 with the controls, GFP and mCherry (Figure 6a, top panels). As in yeast two-

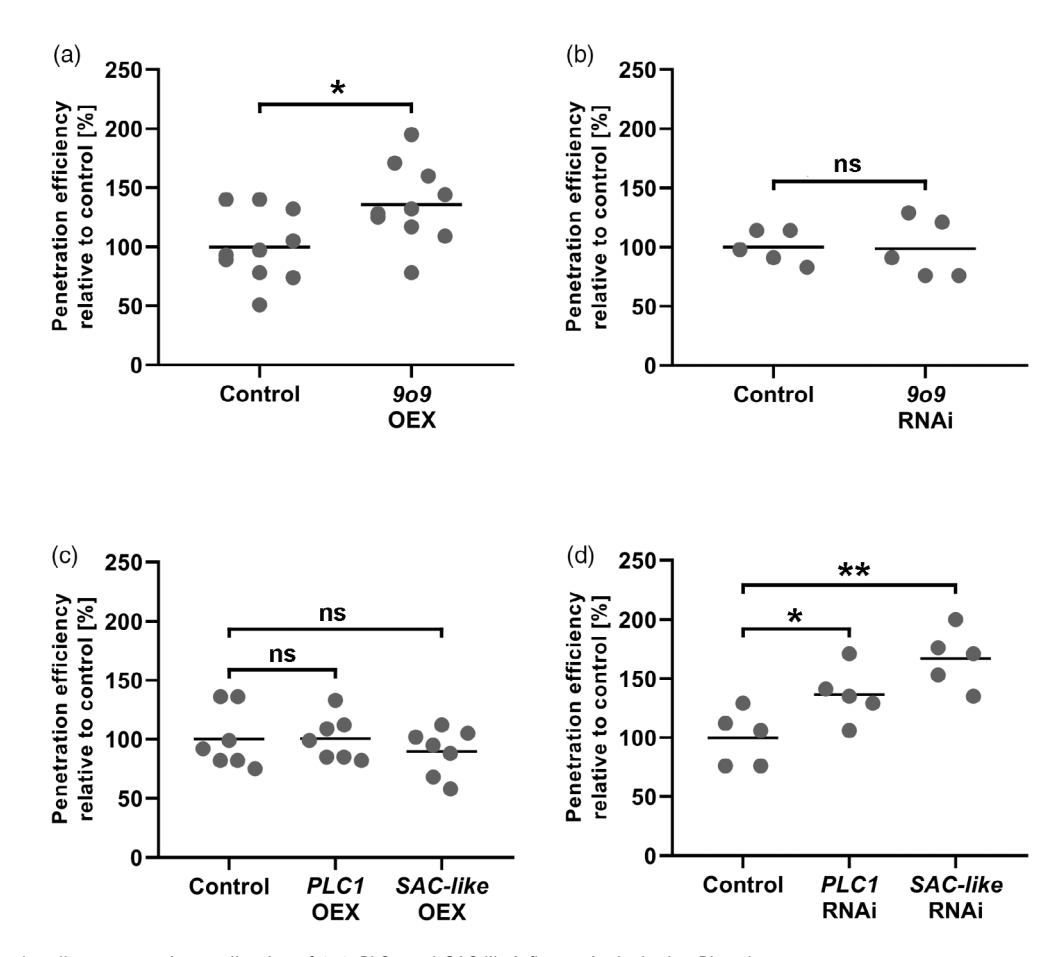


Figure 4. Single-cell overexpression or silencing of 909, PLC1, and SAC-like influence in the barley-Bh pathosystem. The susceptibility of barley epidermal cells toward penetration by Bh was investigated after transient overexpression (a, c) or RNAi-mediated silencing (b, d) of 909, PLC1, and SAC-like at 40 hpi. The respective empty vectors were used as controls. Overexpression of 909 and silencing of PLC1 and SAC-like led to increased susceptibility, whereas silencing of 909 and overexpression of PLC1 and SAC-like showed no influence. RNAi-silencing specificity was confirmed using the si-Fi RNAi-off-target prediction tool (Lück et al., 2019). Each datapoint shows the Bh penetration efficiency of a single experiment relative to its averaged empty vector control. Crossbars display the average susceptibility from 10 (a), five (b, d) and seven (c) independent biological experiments. Statistical differences were calculated with two-tailed Student's t-tests comparing an overexpression or silencing construct with its respective empty vector control: ns P > 0.05, \*P < 0.05, \*\*P < 0.01. OEX: overexpression.

hybrid experiments (Figure 6b) and in FRET-FLIM experiments (Figure 6c), RACB-CA-5Q interacted with RIC171 in a similar manner as the parental RACB-CA; we conclude that lipid binding through the PBR is required for PM association of RACB-CA and for its capability to co-recruit the ROP scaffold RIC171 to the cell periphery upon infection.

Finally, we tested if the RACB-CA-5Q substitution variant is still functional as a susceptibility factor in the barley-Bh pathosystem. Using transient overexpression of regular RACB-CA or RACB-CA-5Q in barley epidermal cells, we detected that the expression of RACB-CA significantly enhanced relative fungal penetration success by 38% compared with empty vector controls (Figure 6d). By contrast, the expression of RACB-CA-5Q reduced fungal penetration success by 15% of control levels. While this decrease was statistically not different from penetration success in empty vector controls, it was significantly lower than that observed upon expression of RACB-CA (Figure 6d). In summary, these experiments showed that the RACB-CA-5Q mutant can still interact with downstream partners, such as RIC171. However, both the subcellular localization and the function of RACB-CA in disease susceptibility are compromised by the substitutions in the PBR that abolish Ptdlns-binding.

# Some anionic phospholipids localize to the site of haustorial invasion by Bh

Since RACB bound to some anionic phospholipids in vitro and this lipid-binding capability was found to be relevant in vivo, we next used fluorescent lipid biosensors to monitor the subcellular distribution of anionic phospholipids, first in untreated barley epidermal cells and then during Bh infection. We chose biosensors for PtdIns4P, PtdIns(3,5)P2, Ptdlns(4,5)P2, or PtdSer for subcellular localization studies

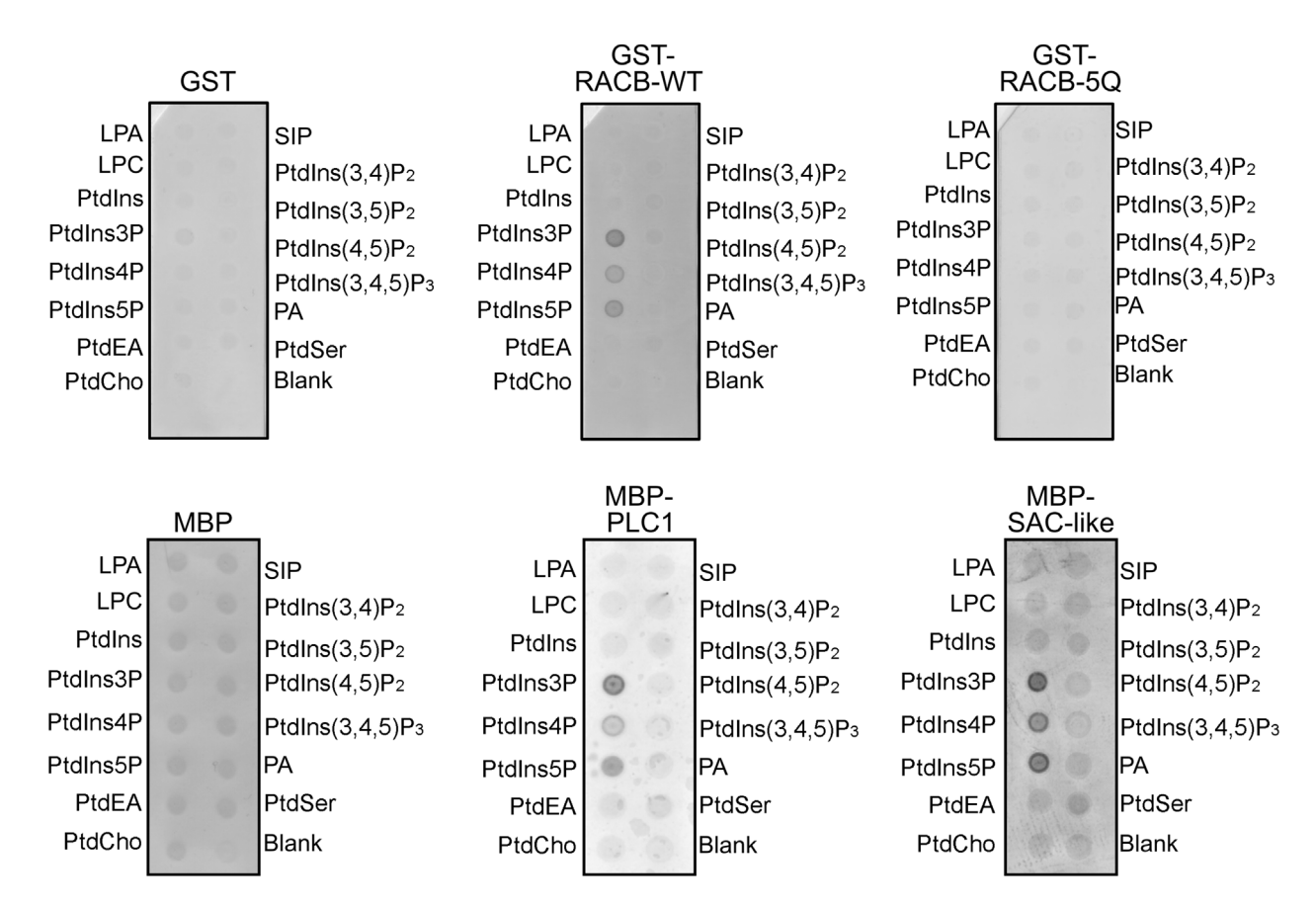


Figure 5. RACB and its candidate interactors associate with PtdIns-monophosphates *in vitro*. RACB and its candidate interactors show lipid-binding in *in vitro* protein–lipid-overlay experiments. Recombinant proteins were purified from *E. coli* using affinity chromatography. Recombinant proteins were incubated with lipid-spotted membranes and detected via α-GST or α-MBP antibodies. Colored dots indicate association with the respective lipid species. Free GST and MBP were used as non-lipid-binding controls. blank: no lipid spotted. LPA, lysophosphatidic acid; LPC, lysophosphatidylcholine; SIP, sphingosine 1-phosphate.

because these lipids had either been linked to ROP signaling before or were shown to display altered behavior during pathogen attack in other plants (Fratini et al., 2021; Hirano et al., 2018; Kost et al., 1999; Platre et al., 2019; Qin et al., 2020). Importantly, in previous reports, Ptdlns(4,5)P<sub>2</sub> has been described as a susceptibility factor for other plant-pathogen interactions (Qin et al., 2020; Shimada et al., 2019). For in planta visualization of the different phospholipids, we used fluorophore-tagged protein domains that bind specific phospholipids (Hirano et al., 2017; Simon et al., 2014). These biomarkers were used for transient transformation of barley epidermal cells that were then observed via CLSM either in non-infected controls (Figure 7a) or during fungal invasion at 16-20 hpi (Figure 7b-e). All biomarkers had to be imaged with individual laser excitation levels and detector gain to detect fluorophore-specific signals. A GFP-2xPHFAPP1 biosensor for PtdIns4P, bound by a double pleckstrin homology (PH) domain of the human Four-Phosphate Adapter Protein (2xPHFAPP1, Simon et al. (2014)), decorated the PM of noninfected barley epidermal cells when compared with

mCherry as a cytoplasmic marker (Figure 7a). The GFP-2xPH<sup>FAPP1</sup> marker also labeled the PM upon Bh attack (Figure 7b). Fluorescence patterns were detectable even though autofluorescence was usually strong in cell wall appositions at sites of attack and overlapping with fluorophore signals (compare Figure 7b,f for a pure autofluorescence signal from an attacked but non-transformed neighbor cell). However, we additionally detected a clear enrichment of the GFP-2xPHFAPP1 marker at the haustorial neck region of successfully Bh-colonized cells, with little autofluorescence at such sites (Figure 7b, see Figure S4 for higher magnification). At sites of successful penetration, signals were strong and originated from the emission  $\boldsymbol{\lambda}$ spectrum of the FAPP1GFP-2xPH-derived GFP signal. Interestingly, the PtdIns4P marker was not detected at the extrahaustorial membrane that is in continuum with the plant PM but of a distinct composition (Kwaaitaal et al., 2017).

A biosensor for PtdIns(4,5)P<sub>2</sub>, a GFP-fused double PH-domain of rat PLC<sub>0</sub>1 (2xPH<sup>PLC</sup>, Simon et al. (2014)), showed a prominent localization at the PM in non-infected cells, with some background signals coming from the cytosol

and nucleus (Figure 7a). By contrast, in Bh-attacked cells, the PM-associated intensity of the GFP-2xPHPLC marker was weaker and became hard to determine, especially due to the intrinsic autofluorescence (Figure 7c). The reduced PM fluorescence was accompanied by an increased cytoplasmic signal for GFP-2xPHPLC (Figure 7c), consistent with a reduction in PtdIns(4,5)P2 at the PM upon Bh attack.

The distribution of PtdIns(3,5)P2 was tracked by mCitrine fused to a tandem repeat of the lipid-binding domain of mammalian Mucolipin 1 (Hirano et al., 2017). The mCitrine-2x-MLN1 marker was visible at the cell periphery, in the nucleus, and in the cytoplasm of non-infected cells (see Figure 7a). While it is difficult to discern from our imaging setup, mCitrine-2x-MLN1 distributed in a pattern differing somewhat from PM localization. Moreover, in some cells, mCitrine-2x-MLN1 fluorescence was also detected in endosomal vesicle-like structures (Figure 7d). As PtdIns(3,5)P<sub>2</sub> has been reported to reside at the plasma membrane, endosomes, and tonoplast (Bak et al., 2013; Hirano et al., 2017: Hirano et al., 2018: Nováková et al., 2014), the observed pattern might represent those localizations. During Bh interaction, the mCitrine-2x-MLN1 marker was present but little distinct at sites of haustorium accommodation and seemingly a bit more enriched around non-penetrated plant cell wall appositions (Figure 7d).

The PS-marker, a GFP-tagged C2-domain of bovine Lactadherin (C2<sup>LACT</sup>, Platre et al. (2018)), was detected mainly at the PM, but also weakly in the cytosol of noninfected barley epidermal cells (Figure 7a). In most cases, the PS-marker was also visible in tiny, potentially vesicular speckles. During Bh infection, GFP-C2<sup>LACT</sup> remained at the PM, but still exhibited a stronger cytoplasmic background signal (Figure 7e) in a similar pattern as the GFP-2xPHPLC marker for Ptdlns(4,5)P<sub>2</sub>. In Bh-colonized cells, a localization at the haustorial neck region was evident for the PSmarker that was more distinct at this position than the cytosolic mCherry signal (Figure 7e, see Figure S4 for higher magnification). Similar to the GFP-2xPHFAPP1 marker for PtdIns4P, the GFP-C2<sup>LACT</sup> marker was also not enriched at the extrahaustorial membrane. In conclusion, the distribution of the various fluorescent biosensors indicates a potential involvement of anionic phospholipids in the barley-Bh interaction, as three of the four lipid biosensors tested (for PtdIns4P, PtdIns(4,5)P2 and for PtdSer) showed an altered localization or subcellular distribution during fungal attack.

Because 909 was originally found in nine Co-IPs with RACB-CA and lipid-modifying PLC1 and SAC-like, we wondered whether 909 could change the subcellular pattern of the tested lipid markers. We found an effect of 909 on the PtdIns(3,5)P<sub>2</sub> marker mCitrine-2x-MLN1. Co-expression of 909 apparently not only supported fungal penetration but also supported the presence of mCitrine-2x-MLN1 at the haustorial neck region (Figure 8).

To gain first hints toward a possible mechanism of 909 action, we wanted to test whether 909 indeed preferentially interacts with activated RACB-CA when compared with wild-type RACB-WT or dominant negative RACB-DN. In targeted Co-IP experiments, we co-expressed HA-tagged HA-909 or 909-HA with GFP-RACB-CA, GFP-RACB-WT, or GFP-RACB-DN in Nicotiana benthamiana. GFP-RACB-DN was not stably expressed in N. benthamiana, but free GFP, GFP-RACB-CA, and GFP-RACB-WT were well detectable in Western blots after precipitation with GFP antibodies. HAtagged versions of 909 co-precipitated with GFP-RACB-CA but neither with GFP-RACB-WT nor free GFP. This supports that 9o9 preferentially interacts with GTP-loaded RACB (Figure S5). Protein complex modeling of protein dimers of GTP-loaded RACB with PLC1, SAC-like, and 9o9 further suggests that all three interaction partners of RACB share an overlapping interface of protein-protein interaction with partially identical amino acids around the ROP effector loop of RACB responsible for binding the respective partner (Figure S5).

#### **DISCUSSION**

## PM association through interaction with PtdInsmonophosphates is essential for RACB function in disease susceptibility

ROPs need to associate with the PM for activation and downstream signaling activities in plant development (Platre et al., 2019; Yalovsky, 2015). Here, we analyzed how the barley RACB protein interacts with the PM, whether it binds membrane phospholipids, and whether this interaction is relevant for its role as a susceptibility factor in the barley-Bh interaction. First, we confirmed previous findings with untagged or HA-tagged versions of RACB that overexpression of full-length PM-localized GFP-RACB-CA increased susceptibility toward Bh infection, whereas a mislocalized cytoplasmic GFP-RACB-CA-ΔCSIL mutant did not support susceptibility (Figure 1b,c; Schultheiss et al., 2003, Weiss et al., 2022). Mechanistically, the RACB-CA-ΔCSIL mutant could be affected in its ability to associate with downstream executors since these interactions are often observed at the PM (Hoefle et al., 2011; McCollum et al., 2020; Schultheiss et al., 2008). Alternatively, it is possible that cytoplasmic RACB-CA-ΔCSIL can interact with downstream executors, but this interaction is spatially separated from usual ROP-signaling processes at the PM. Irrespective, both the subcellular localization of RACB and its activation status appear essential for RACB function in susceptibility. The ability to interact with phospholipids can also influence the subcellular localization and associated signaling capacities of ROPs, such as the type I ROP AtROP6 or the type II ROP AtROP11 (Platre et al., 2019;

1363313x, 2025, 2, Downloaded from https://onlinelibrary.wiley.com/doi/10.1111/tpj.70356 by Martin Luther University Halle-Wittenberg, Wiley Online Library on [16/10/2025]. See the Terms

litions) on Wiley Online Library for rules of use; OA articles are governed by the applicable Creative Commons Licenso

Figure 6. RACB-CA localization and function depend on positively charged amino acid residues in its PBR.

(a) The subcellular localization of GFP-tagged RACB-CA or its derivate RACB-CA-5Q together with its mCherry-tagged putative downstream scaffold protein RIC171 were investigated via CLSM after transient transformation of epidermal cells. Size bars represent 50 µm.

(b) Yeast two-hybrid assay of binding domain (Vossen *et al.*) tagged RACB-variants (WT, wild-type; CA, constitutively activated; DN, dominant negative) with activation domain (AD) tagged RIC171 in yeast on protein interaction non-selective complete supplement medium (CSM) plates lacking leucine and tryptophan (-L -W) or protein interaction selective plates lacking leucine, tryptophan, histidine, and adenine (-L -W -H -Ade), or protein interaction selective plates supplemented with 0.5 mm 3-aminotriazole (-L -W -H + 0.5 mm 3-AT). Interaction indicative growth is visible for combinations between RIC171 and each of RACB-WT, RACB-WT-5Q, RACB-CA, and RACB-CA-5Q. Interaction between T-antigen and p53 served as a positive control for the yeast two-hybrid experiment.

(c) Interaction of GFP-tagged versions of RACB-CA with mCherry-RIC171 in FRET-FLIM experiments. Barley epidermal cells were transiently transformed via particle bombardment with expression constructs for either GFP-RACB-CA or GFP-RACB-CA-5Q as FRET-donors and mCherry-RIC171 as a FRET acceptor. Free mCherry served as no-interaction controls. FRET-FLIM measurements were conducted at the cell periphery of the equatorial plane of barley epidermal cells 2 days after transformation. Stars display statistically significant differences between the samples (Tukey test, ns P > 0.05, \*\*P < 0.01, \*\*\*P < 0.001, \*\*\*\* P < 0

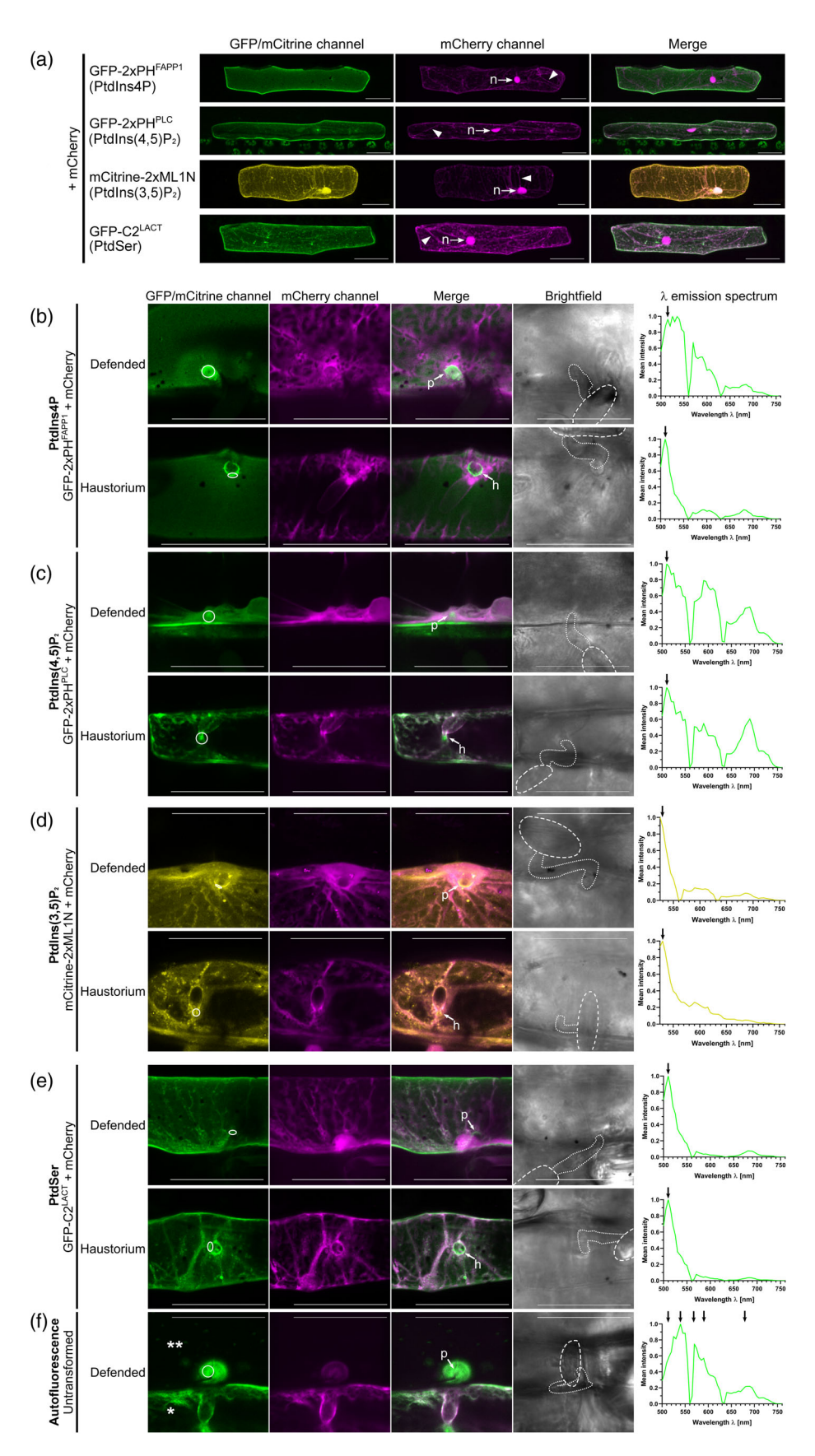
(d) The susceptibility of barley epidermal cells toward penetration by Bh was investigated after transient overexpression of RACB-CA or RACB-CA-5Q or an empty vector control, respectively. Each data point shows the Bh penetration efficiency of a single experiment relative to its averaged control. Crossbars display the average susceptibility from four independent biological experiments. Statistical differences were calculated with Tukey test, ns P > 0.05, \*\*P < 0.01, \*\*\*P < 0.01 based on an ANOVA (significant at  $\alpha = 0.05$ ). Control = empty vector transformation.

Sternberg et al., 2021). AtROP6, a type I ROP similar to RACB, associates with PtdSer and with PtdInsmonophosphates (Platre et al., 2019). In planta, PtdSer is essential for enrichment of AtROP6-CA in PM nanodomains (Platre et al., 2019). By contrast, AtROP6-7Q did not cluster in nanodomains, accompanied by abolished signaling capacity (Platre et al., 2019). Data presented here indicate that barley RACB also interacts with different PtdInsmonophosphates in vitro (Figure 5), and this lipid interaction was important for subcellular localization at the PM (Figure 6a) and for the role of RACB as a susceptibility factor during the barley-Bh interaction (Figure 6d). Our experiments show that an interaction between ROPs and Ptdlns-monophosphates can support compatible plantpathogen interactions. Additionally, it was shown earlier that the PBR of ROPs is also required for efficient prenylation of CaaX-box motifs (Caldelari et al., 2001), such that failure of RACB-CA-5Q may arise from a combination of effects. In analogy to AtROP6 (Platre et al., 2019), activated barley RACB might enrich in PM-domains in a phospholipid-dependent manner. As the lipid-binding-deficient RACB-CA-5Q protein could still interact with the scaffold protein RIC171 in yeast and in planta, most likely protein mislocalization rather than protein misfolding was responsible for the failure of RACB-CA-5Q to recruit signaling partner proteins to the PM or to function as a susceptibility factor. Our data indicate that the function of RACB as a susceptibility factor requires PM localization, which is mediated by both CSIL prenylation (Schultheiss et al., 2003; Weiss et al., 2022) and the binding to PtdIns-monophosphates and possibly other anionic phospholipids through positively charged lysine residues in its PBR.

# 909 Is a Bh-effector protein targeting activated RACB

The untargeted RACB-CoIP from *Bh*-infected epidermal peels of barley plants identified 909, a putative effector protein from *Bh*, as a candidate RACB-CA interaction partner, and the 909-RACB-CA interaction could be verified by

a range of other methods. The Bh 909 protein belongs to the CSEP superfamily of Blumeria spec. effectors (Figure S3a; Pedersen et al., 2012) that contain many validated effector proteins with functions in effector-triggered susceptibility and effector-triggered immunity. However, with 317 amino acids in length, 909 is more prominent in size when compared with most characterized Blumeria effector proteins. In planta interaction of 909 with RACB-CA (Figure 2a; Figure S5) might be part of a potential virulence mechanism for 909, since exploiting susceptibility factors is a virulence strategy for several pathogens (Choi et al., 2021; He et al., 2018; Mackey et al., 2002). The expression of the 909 gene is strongly upregulated during the early stages of Bh invasion (Figure 3a), and transient overexpression of 909 in barley increased susceptibility toward Bh invasion (Figure 4a). Our effort to prove the physiological function of 909 by host-induced gene silencing was not successful. This may be explained by the redundancy of 9o9 and other similar effectors or dissimilar effectors potential targeting of the same host pathway. This seems possible because B. hordei actually expresses hundreds of effector candidates, which may overwhelm host countermeasures but make single effectors genetically dispensable (Pedersen et al., 2012; Spanu et al., 2010). Interestingly, 9o9 is not the only effector protein targeting activated RACB. The effector, Bh ROP-INTERACTIVE PEPTIDE 1 (ROPIP1), is an unconventional effector encoded by a transposable element and was previously found to interact with RACB, resulting in the fragmentation of microtubules in the host cell, a process associated with susceptibility to fungal invasion (Huesmann et al., 2012; Nottensteiner et al., 2018). The finding that RACB is a potential target of two diverse effector proteins highlights the importance of RACB for the infection success of Bh. We currently can only speculate how 909 might manipulate RACB functions. In this context, it is worth noting that RACB function in cytoskeletal organization and cell polarity might be important for defense, too,



1365313x, 2025. 2. Downloaded from https://onlinelibrary.wiley.com/doi/10.1111/tpj.70356 by Martin Luther University Halle-Wittenberg, Wiley Online Library on [16/10/2025]. See the Terms and Conditions (https://onlinelibrary.wiley

-and-conditions) on Wiley Online Library for rules of use; OA articles are governed by the applicable Creative Commons

(b-f) Images of infected cells were taken between 16 and 20 hpi. High-magnification images of non-penetrated ("Defended") and Bh-colonized ("Haustorium") cells are shown. Arrows point to unsuccessful penetration attempts (p) or haustorial entry points (h). PtdIns4P (b) and PtdSer (e) were enriched at the haustorial neck region of Bh-colonized cells. Signal from Ptdlns(4,5)P2 (c) was primarily visible in cytosol and nucleus, but was hard to evaluate due to very low fluorescence levels. Ptdlns(3,5)P<sub>2</sub> (d) was slightly enriched at the cell wall apposition of non-penetrated cells. The circles in the GFP/mCitrine-images show regions-ofinterest that were λ-scanned to evaluate fluorescence emission spectra. λ-scanning was performed in 5 nm detection steps after excitation with a 488 nm (GFP) or 514 nm (mCitrine) laser source. Only in non-penetrated GFP-2xPH<sup>FAPP1</sup>-transformed cells and all GFP-2xPH<sup>PLC</sup>-transformed cells, a strong presence of non-GFP-signals could be detected that was likely autofluorescence emitted by phenolic compounds released during plant defense responses. In all other cells, spectra matched that of GFP or YFP (fluorophore emission maxima are highlighted by arrows:), For reference, (f) shows both autofluorescence in an untransformed. Bh-attacked cell (\*\*) and, side by side, a single transformed cell (\*) imaged with the settings for Ptdlns(4,5)P2. \(\lambda\)-scanning was performed in the indicated region of interest (circle) to characterize autofluorescence emitted during high laser excitation levels and detector gain. Note the lack of the typical GFP peak around 510 nm and the peaks/shoulders from autofluorescence at about 540, 570, 590, and 690 nm. Free mCherry was co-transformed as a marker for cytosolic and nuclear fluorescence. All images except brightfield pictures show Z-stack maximum intensity projections of at least 4 XY-optical sections captured in 1.5 μm Zsteps. Brightfield images show single XY-optical sections, in which spores are outlined with dashed lines and appressoria are highlighted with dotted lines. Scale bar: 50 µm. Representative images from at least five events in each of at least two independent biological replicates are shown. All images were taken with individual laser excitation strength and detector gain for higher image clarity. Image brightness was uniformly enhanced post-scanning for better visibility.

because both processes have been shown to act in penetration resistance to diverse fungal pathogens (Schmelzer, 2002). It is possible that Bh takes advantage by abusing RACB function in cell polarity for redirecting transport processes toward material delivery for the formation of the haustorial complex, which depends on host-derived extrahaustorial matrix and membrane materials.

#### PLC1 and SAC-like work in resistance against Bh

Besides 909, we also identified barley PLC1 and SAC-like as RACB interactors in the RACB-CoIP experiment, and proteins were enriched in untreated or Bh-infected samples of the CoIP-LC-MS/MS screening, respectively. During Bh infection, PLC1 and SAC-like were not differentially expressed over the first 24 h of host colonization (Figure 3b,c). However, both proteins have roles in supporting resistance against powdery mildew infection, as the penetration frequency of Bh increased upon transient RNAi-mediated silencing of gene expression (Figure 4d). Both PLC1 and SAC-like are phosphoinositide-degrading enzymes, and their suppression likely contributes to the delimitation of phosphoinositide abundance. As phosphoinositides, such as PtdIns(4,5)P2, have been identified as susceptibility factors in different plant-pathogen interactions (Qin et al., 2020; Shimada et al., 2019), enhanced phosphoinositide abundance could explain the increased susceptibility to Bh observed as a consequence of suppression of PLC1 and/or SAC-like in barley epidermis cells (Figure 4d). It is interesting to see two enzymes of phosphoinositide degradation interact with RACB-CA in barley, adding to several other reported modes of limiting the abundance of phosphoinositides during plant defense, including the posttranslational inhibition of Arabidopsis PIP5K6 (Menzel et al., 2019) or the transcriptional activation of a gene encoding a phosphoinositide 5-phosphatase in

potato in response to different PAMP treatments (Rausche et al., 2021). With regard to ROP signaling, canonical RACB-downstream interactors are often connected to powdery mildew susceptibility (Engelhardt et al., 2023; McCollum et al., 2020; Schultheiss et al., 2008). Other RACB-interacting proteins function in resistance against Bh and have been suggested to negatively regulate RACBsignaling processes. mediated instance, MICROTUBULE-ASSOCIATED ROP GTPase ACTIVATING PROTEIN1 likely inhibits RACB signaling through its GTPhydrolyzing GAP function, whereas ROP BINDING KINASE1 and the E3 ubiquitin ligase subunit SKP1L negatively regulate RACB protein abundance (Hoefle et al., 2011; Huesmann et al., 2012; Reiner et al., 2016). PLC1 and SAC-like might antagonize RACB signaling via their predicted phospholipid-degrading activities, possibly limiting PM association of RACB. Signaling pathways of RACB, PLC1, and SAC-like could converge on phosphoinositides because all three proteins can bind similar lipid species in vitro (Figure 5). During Bh attack, some anionic phospholipid species enrich at the site of fungal attack (Figure 7) and thereby potentially recruit RACB in a similar manner as proposed for AtROP6 in Arabidopsis (Platre et al., 2019). Focal accumulation could subsequently support RACB signaling processes that lead to Bh susceptibility. However, enzymatic activity of PLC1 and SAC-like could degrade accumulating anionic phospholipids that would antagonize membrane polarization and related RACB signaling in susceptibility. In animals, activation of PLCs by RACB-like Rho proteins has been shown (Jezyk et al., 2006; Li et al., 2009; Rao et al., 2008). In plants, however, PLCs are activated by Ca<sup>2+</sup> (Pokotylo et al., 2014), whereas little is known about the modes of regulation of SACs. PLC proteins were shown to be heat stress responsive and to govern drought and salt stress responses in

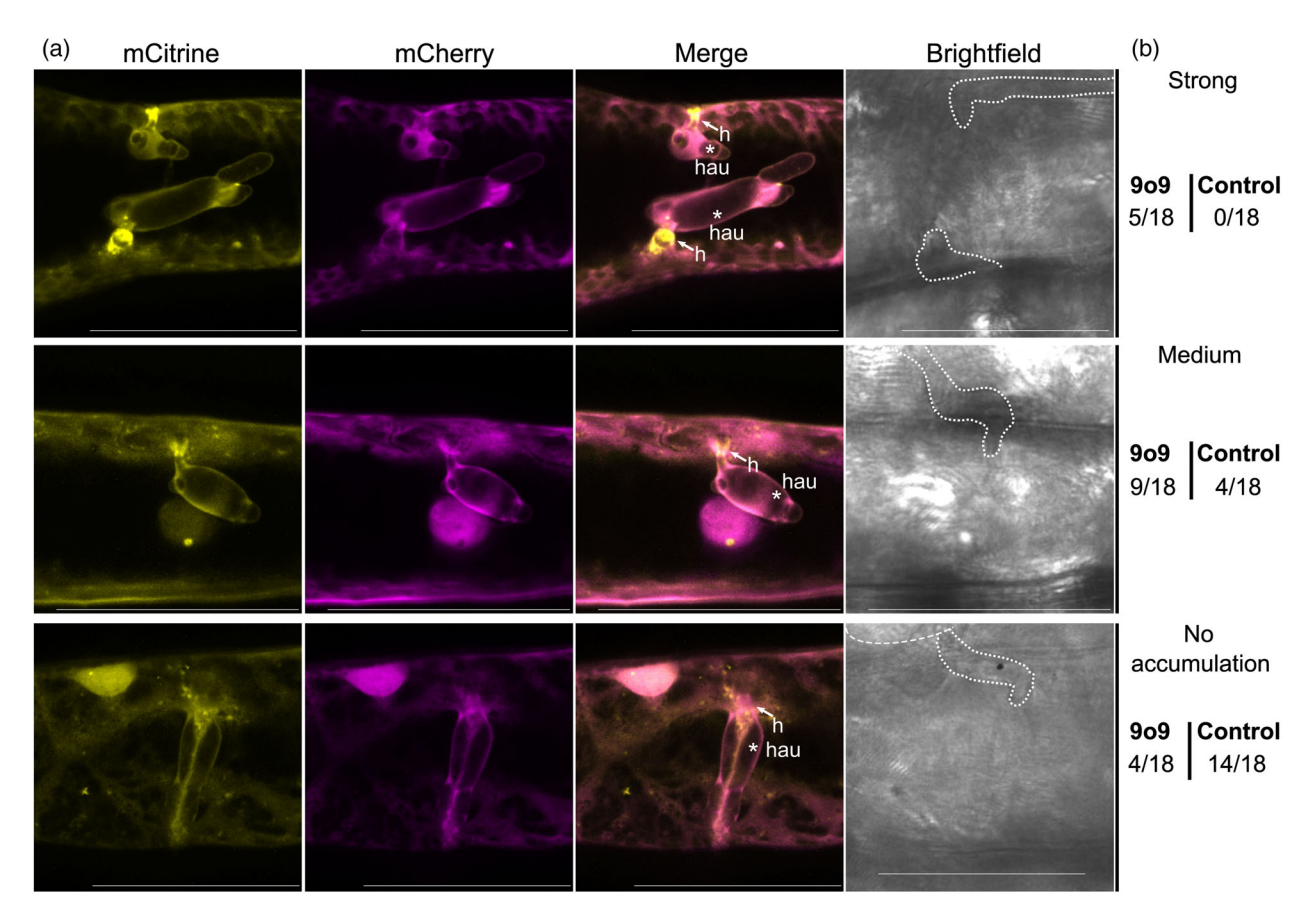


Figure 8. Effect of 909 on the subcellular localization of Ptdlns(3,5)P<sub>2</sub> marker in *Bh*-infected barley epidermal cells.

(a) The subcellular localization of the anionic phospholipid Ptdlns(3,5)P<sub>2</sub> was analyzed in barley epidermal cells via confocal laser scanning microscopy following transient co-transformation with *Bh* 909 and the Ptdlns(3,5)P<sub>2</sub>-specific biosensor Citrine-2x-ML1N (Hirano et al., 2017). Free mCherry was co-transformed as a cytosolic marker. Images of infected cells were taken between 16 and 20 hpi. High-magnification images of *Bh*-colonized cells are shown; haustorial entry points are indicated with (h) and the asterisk (\*) indicates the haustorial body. All images show Z-stack maximum intensity projections composed of at least 16 XY-optical sections captured in 1.5 μm Z-steps. Brightfield images represent single sections of the transmission channel, with the haustorium out of focus. Scale bar: 50 μm. Image brightness was uniformly enhanced post-acquisition for better visualization. Representative images illustrate three categories of Ptdlns(3,5)P<sub>2</sub> accumulation at haustorial entry sides/neck region: strong accumulation (upper panel), medium accumulation (middle panel), and no accumulation (lower panel).

(b) Counting of Ptdlns(3,5)P<sub>2</sub> accumulation patterns observed in each of 18 cells expressing 909 or control cells co-transformed with the empty vector. In 909-expressing cells, Ptdlns(3,5)P<sub>2</sub> accumulation at haustorial entry points was seen in the majority of cells. In most control cells, Ptdlns(3,5)P<sub>2</sub> accumulation was absent or weak.

different plant species (Georges et al., 2009; Liu et al., 2006; Tripathy et al., 2011; Wang et al., 2008). In biotic interactions, tomato PLC6 was shown to be important for defense against the fungi *Cladosporium fulvum* and *Verticillium dahliae*, and the bacterium *Pseudomonas syringae* (Vossen et al., 2010). In rice, gene expression of *OsPLC1*, the closest homolog of barley PLC1 (Figure S4b), was shown to be stimulated by chemical and biological signals from the systemic acquired signaling pathway (Song & Goodman, 2002). In summary, these studies about different PLCs are consistent with a possible role of barley PLC1 in resistance to fungal pathogens. For proteins from the SAC family, studies were conducted with regard to endomembrane trafficking and organelle morphology (Mao & Tan, 2021; Nováková et al., 2014).

# Dynamic asymmetric distribution of anionic phospholipids in barley cells during *Bh* attack

Since we found phospholipid-binding abilities for RACB and its novel interaction partners, we also investigated the subcellular localization of anionic phospholipid markers in barley during *Bh* attack. In *Bh*-infected barley epidermal cells, the plasma membrane-localized PtdIns4P and PtdSer biomarkers were found enriched at the haustorial neck region but were excluded from the plant extrahaustorial membrane (Figure 7b,e; Figure S4), whereas a biomarker for PtdIns(4,5)P<sub>2</sub> was displaced from the PM during fungal attack (Figure 7a,c). Some of our data match results from other plant pathosystems, in which the subcellular distribution of different anionic phospholipid species was

investigated. For instance, in Arabidopsis, a PtdIns4P biomarker was found at the haustorial neck region during infection by the oomycete, Hyaloperonospora arabidopsidis (Hpa) or by the powdery mildew fungus Erysiphe cichoracearum (Ec) (Qin et al., 2020; Shimada et al., 2019). In both pathosystems, the PtdIns4P marker was also excluded from the extrahaustorial membrane. In Arabidopsis, markers for PtdIns(4,5) P<sub>2</sub> appear enriched at the extrahaustorial membrane of Hpa, Ec, and Golovinomyces orontii (Go) or the extra-invasive hyphal membrane of Colletotrichum higginsianum (Qin et al., 2020, Shimada et al., 2019), but were not clearly detected at comparable structures in barley epidermal cells. However, displacement of a Ptdlns(4,5)P<sub>2</sub>-marker from infection structures was previously observed in potato plants infected by Phytophthora infestans (Rausche et al., 2021). Several anionic phospholipid species have previously been linked to ROP signaling. PtdSer is required for the auxin-induced partitioning of AtROP6 into PM nanodomains during root gravitropism in Arabidopsis (Platre et al., 2019), whereas Ptdlns(3.5)P<sub>2</sub> might contribute to governing cell wall hardening in Arabidopsis root hairs together with the type II ROP, AtROP10 (Hirano et al., 2018). Ptdlns(4,5) P2 mediates root hair positioning and polar growth in Arabidopsis together with the RACB-related type I ROPs, AtROP2 and AtROP6 (Hirano et al., 2018; Jones et al., 2002; Kusano et al., 2008; Stanislas et al., 2015), and it also regulates the actin cytoskeleton during Nicotiana tabacum (Nt) pollen tube growth via the type I ROP, NtRAC5 (Fratini et al., 2021; Kost et al., 1999). In pollen tubes, Ptdlns(4,5)P<sub>2</sub> even stimulates the activation of ROPs, likely by interfering with the ROP interaction with GDP-dissociation inhibitors, which otherwise sequester ROPs in the cytoplasm and limit their activation at the PM (Fratini et al., 2021; Ischebeck et al., 2011; Kost, 2008). Together, the available information leads us to propose that anionic phospholipids serve as positional membrane signals for the PM recruitment of RACB and associated proteins to enable RACBmediated susceptibility. This is supported by the lipiddependent PM association of RACB and RACB-supported plasma membrane association of its three canonical interactors RIC157, RIC171, and RIPb. When co-expressed during Bh infection, RACB-CA and either of the three scaffold proteins co-localize at the haustorial neck region (Engelhardt et al., 2023; McCollum et al., 2020; Schultheiss et al., 2008) in a manner similar to what we observed for fluorescent reporters for PtdSer and particularly for PtdIns4P. Both RICs and RIPb contain polybasic stretches in their amino acid sequences, which possibly enable them to bind anionic phospholipids (Engelhardt et al., 2023, McCollum et al., 2020, Schultheiss et al., 2008).

The question arises how 909 might mechanistically support virulence by targeting RACB. Possibly an effector could influence RACB stability, GTP hydrolysis, or the GDP

for GTP-exchange of the ROP GTPase. Our protein complex modeling suggested that 9o9 binds to a set of surface amino acids in RACB that overlapped with RACB-PLC1 and RACB-SAC-like contact amino acids in the ROP effector loop that is also responsible for ROP regulators and downstream proteins (Figure S5). Although modeling-based prediction has to be taken with care, one might hence speculate that B. hordei 909 competes with host proteins, which act in defense, for binding to RACB. Such competition could limit recruitment of antagonistic ROPGAPs or of PLC1 or SAC-like to the site of fungal attack. Since SAC-like is similar to SAC proteins that might act on Ptdlns(3,5)P<sub>2</sub>, our observation that 9o9 supports accumulation of the Ptdlns(3,5)P2-marker at the haustorial neck region could reflect displacement of barley SAC-like by fungal 909 leading to changes in the amount or subcellular distribution of Ptdlns(3,5)P<sub>2</sub>. However, further experimental support is required to underpin this possible explanation. Ptdlns(3,5) P<sub>2</sub> is partially found on plant endosomes (Hirano et al., 2017; Noack & Jaillais, 2020). Possibly, 9o9 supports redirection of endosomes to the haustorial neck region or hinders early enough redirection during defense of fungal penetration attempts. In this context, it is interesting that host endomembrane trafficking is crucial for plant defense and a target of other B. hordei effectors that suppress barley immunity (Liao et al., 2023; Nielsen, 2024; Sabelleck et al., 2025). In conclusion, we suggest that during Bh infection anionic phospholipids enrich at infection sites and interact with susceptibility factors, such as RACB, which facilitates susceptibility toward Bh infection and supports ingrowth of the fungal haustorium into the intact host cell. Simultaneously, RACB and anionic phospholipids may recruit phospholipid-metabolizing enzymes that function to spatially restrict phospholipid functions or membrane domains, and this might limit fungal infection success. Future studies may help to better understand the spatiotemporal order of lipid- and ROP-signaling events and the mechanistic detail of their interconnection.

#### **EXPERIMENTAL PROCEDURES**

#### Molecular cloning

Cloning of all constructs from this study was achieved by a combination of classical cloning, Gateway® and GoldenGate techniques. Please see File S1 and Table S2 for a detailed description of all cloning processes and primers.

## Plant and fungal growth conditions

Wild-type barley (Hordeum vulgare L. subspecies vulgare) plants cultivar Golden Promise and transgenic barley lines were grown in a climate chamber (Conviron, Winnipeg, Canada) at 18°C, 65% relative humidity and a cycle of 16 h of 150 μm s<sup>-1</sup> m<sup>-2</sup> light followed by 8 h dark. All experiments with transgenic plants used transgene-expressing individuals of generation T2 (see below; lines BG654 E02 and E12 for eGFP-RACB-CA, BG655 E01 and E10

for eGFP-RACB-CA- $\Delta$ CSIL and BG656 E01 and E06 for eGFP), with one exception: for the analysis of the Bh susceptibility of transgenic plants, transgene-expressing offspring of generation  $T_1$  were used because the  $T_2$  plants were not ready at the time. The barley powdery mildew fungus  $Blumeria\ hordei$  isolate A6 (Bh) was cultivated on Golden Promise under the same conditions. All experiments used Bh-infected plants between 7 and 9 dpi as inoculum.  $Nicotiana\ benthamiana$  plants were sown on a mixture of 1 part vermiculite (1/3 mm; Raiffeisen Gartenbau, Köln, Germany) and 5 parts soil, then stratified for >2 days at 4°C before being grown under long-day conditions (55% relative humidity, 16 h 150  $\mu$ M s $^{-1}$  m $^{-2}$  light at 23°C, 8 h dark at 21°C).

#### Generation and selection of transgenic barley lines

The transgenic barley lines from this study were created similarly to those described in Weiss et al. (2022). Please see File S1 for a detailed description of the method.

#### **Immunoprecipitation**

First leaves were frozen in liquid N2 and homogenized using a mortar and pestle for protein IPs from transgenic barley plants. Proteins were extracted using 400 ul extraction buffer (10% (w/v) glycerol. 25 mm Tris pH 7.5, 1 mm EDTA, 150 mm NaCl, 10 mm DTT, 1 mm PMSF, 0.5% Nonidet P40 substitute, 1x protease inhibitor [P9599; Sigma-Aldrich, St. Louis, MO, USA]) and a 30 min incubation on ice, followed by removing cell debris via 10 min centrifugation at 4°C and 18 000 g. For targeted CoIPs from transiently transformed Nicotiana benthamiana plants, five leaf discs (1.2 mm diameter) were taken with a biopsy puncher, frozen in liquid N2 and homogenized using a TissueLyser II (QIAGEN, Hilden, Germany). Proteins were extracted in 500 µl extraction buffer and cell debris was removed as described above. Immunoprecipitation from debriscleared supernatants of barley or Nicotiana benthamiana samples was conducted according to standard methods. For one α-GFP IP, 10 μl GFP-Trap® magnetic agarose beads (gtma-10; Chromotek, Planegg, Germany) were used (20 µl/sample for interactome samples). Briefly, beads were equilibrated three times with 400  $\mu$ l extraction buffer. After adding supernatants, samples were tumbled end-over-end for 1 h at 4°C, then washed 5 times with washing buffer (10% (w/v) alveerol, 25 mm Tris pH 7.5, 1 mm EDTA, 150 mm NaCl, 1 mm PMSF, 1× protease inhibitor [P9599; Sigma-Aldrich]). Proteins were eluted in either 50  $\mu$ l 2 $\times$  SDS-loading dye (for routine IPs; 40% (w/v) glycerol, 200 mm Tris-HCl pH 6.8, 20% β-Mercaptoethanol, 8% (w/v) SDS, 0.02% (w/v) bromophenol blue;) or 100 µl 2× NuPAGE™ LDS Sample Buffer (for the epidermis interactome; NP0008; Thermo Fisher Scientific, Waltham, MA, USA) and boiled at 95°C for 20 min. In case that additional fractions apart from the IP eluate were needed, 12.5  $\mu l$  of 4 $\times$  SDS-loading dye were mixed and boiled with 37.5 µl of samples taken after protein extraction ("Input"), incubation with the tag-specific beads ("Unbound") or the last washing step ("Wash"). All samples were analyzed via routine SDS-PAGE and α-GFP Western blotting or α-GFP/α-HA Western blotting for Co-IP-analysis. Interactome samples were instead used for peptide identification via mass spectrometry. All antibodies can be found in Table S4.

#### Preparation of the barley epidermis RACB-interactome

This experiment used pools of transgene-expressing plants in generation  $T_2$  for eGFP-RACB-CA (lines BG654 E02 and E12), eGFP-RACB-CA- $\Delta$ CSIL (lines: BG655 E01 and E10) and eGFP (BG656 E01 and E06). For the epidermis interactome, three biological replicates were prepared per construct (eGFP, eGFP-RACB-CA or eGFP-RACB-CA- $\Delta$ CSIL) and condition (*Bh*-infected or mock).

One biological replicate consisted of three technical replicates. For one technical replicate of the "inoculated" condition, 21 primary leaves belonging to one construct were placed on 0.8% wateragar plates with the abaxial leaf side facing up. These plates were challenge-inoculated with 100–130 Bh spores/mm² and put under normal growth conditions for 24 h. For the "mock" condition, the same approach without inoculum was used. After 24 hpi, abaxial epidermal peels were produced, pooled in one tube, and stored in liquid nitrogen until homogenization. All interactome samples were homogenized using a TissueLyser II (QIAGEN) and proteins were resuspended in 400  $\mu l$  extraction buffer before being used in  $\alpha\text{-GFP}$  immunoprecipitations.

#### Mass spectrometry

Interactome IP eluates in LDS sample buffer were reduced with 10 mm dithiothreitol (DTT) for 1 h, followed by alkylation with 55 mm chloroacetamide (CAA) for 30 min at room temperature. Samples were run into a 4-12% NuPAGE gel (Invitrogen, Carlsbad, CA, USA) for approximately 1 cm. Samples from the same biological replicate and treatment condition were run together on one gel. In-gel digestion followed standard procedures with trypsin (Roche, Basel, Switzerland) and TEAB digestion Digested peptides were analyzed by chromatography-coupled mass spectrometry (LC-MS/MS) analysis on Orbitrap mass spectrometers (Thermo Fisher Scientific) coupled online to a Dionex 3000 HPLC (Thermo Fisher Scientific). The liquid chromatography setup consisted of a 75  $\mu m \times 2 \ cm$ trap column packed in-house with Reprosil Pur ODS-3 5 μm particles (Dr. Maisch GmbH, Ammerbuch, Germany) and 75  $\mu$ m  $\times$  40 cm analytical column packed with 3  $\mu$ m particles of C18 Reprosil Gold 120 (Dr. Maisch GmbH), Peptides were loaded onto the trap column using 0.1% FA in water. Measurements were performed on a Q Exactive HF-X (Thermo Fisher Scientific). Separation of the peptides was performed by using a linear gradient from 4 to 32% ACN with 5% DMSO and 0.1% formic acid in water over 20 min, followed by a washing step (30 min total method length) at a flow rate of 300 nl/min and a column temperature of 50°C. The instrument was operated in data-dependent mode, automatically switching between MS and MS2 scans. Full-scan mass spectra (m/z 360-1300) were acquired in profile mode with 60 000 resolution, an automatic gain control (AGC) target value of 3e6, and 45 ms maximum injection time. For the top 12 precursor ions, high-resolution MS2 scans were performed using HCD fragmentation with 26% normalized collision energy, 15 000 resolution, an AGC target value of 2e5, 25 ms maximum injection time, and 1.3 m/z isolation width in centroid mode. The minimum AGC target value was set to 2.2e3, with a dynamic exclusion of 20s. Peptide identification and quantification were performed with MaxQuant (Cox & Mann, 2008) using standard settings (V1.5.8.3). Raw files were searched against a barley database (Morex V2, 160517\_Hv\_IBSC\_PGSB\_r1\_proteins\_HighConf\_REPR\_annotation.fasta: IPK Gatersleben: Mascher et al., 2017) and common contaminants. The recombinant protein sequences and a barley powdery mildew reference database (Blumeria hordei isolate DH14, uniprot-proteome\_UP000015441, Frantzeskakis et al. (2018)) were added to the search space. Carbamidomethylated cysteine was set as a fixed modification, and oxidation of methionine, N-terminal protein acetylation, phosphorylation of serine, threonine, or tyrosine, and GlvGlv modification of lysine were set as variable modifications. Trypsin/P was specified as the proteolytic enzyme, with up to two missed cleavage sites allowed. The match between run function was enabled but restricted to either control or barley powdery mildew-treated samples. Results were filtered to 1% PSM, protein, and Site FDR. Resulting data from MaxQuant was imported into Perseus V1.5.5.3 (Tyanova et al., 2016) for statistical analysis. Significant enrichment of peptides was calculated using two-tailed Student's t-tests against an  $\alpha$  of 0.05. Data was then imported into Microsoft Excel 2016 (Microsoft, Redmond, WA, USA) for the identification of novel eGFP-RACB-CA interaction partners. The considered criteria were statistically significant enrichment or exclusive presence in eGFP-RACB-CA samples. degree of enrichment, and number of unique peptides. The mass spectrometry proteomics data have been deposited to the ProteomeXchange Consortium via the PRIDE (PMID: 34723319) partner repository with the dataset identifier PXD056811.

#### Transient transformation of *Nicotiana benthamiana* plants

Nicotiana benthamiana plants were transformed via Agrobacterium tumefaciens (strain GV3101 pMP90; Lazo et al. (1991)) with a protocol adapted from Yang et al. (2000). Please see File S1 for a complete description.

#### Transient transformation of barley

Epidermal cells of WT barley cv. Golden Promise leaves were transiently transformed via particle bombardment with a protocol adapted from (Schweizer et al., 1999). See File S1 for a comprehensive description.

#### Analysis of Bh penetration efficiency

The Bh susceptibility assessment of transgenic plants was conducted in lines BG654 E2 for eGFP-RACB-CA, BG655 E1 for eGFP-RACB-CA-ΔCSIL and BG656 E1 for eGFP, as described in Weiss et al. (2022). All plants were selected transgene-expressing offspring in generation T<sub>1</sub>. Bh susceptibility of transiently transformed barley plants was performed as described in Engelhardt et al. (2023). For a comprehensive description, see File S1.

## Confocal laser scanning microscopy

For subcellular localization experiments, barley leaf epidermis was transiently transformed as described above and imaged at 24 h after transformation (hat). In case of Bh infection, transformed barley leaves were inoculated with 100-130 Bh spores/mm<sup>2</sup> at 8 hat and imaged at 16-20 hpi unless indicated otherwise. All subcellular localization experiments were performed with a Leica (Wetzlar, Germany) TCS SP5 mounted on a DM6000 stage. All images were taken with a HCX PL APO lambda blue 20.0 × 0.7 IMM UV objective (Leica, Wetzlar, Germany). CFP was excited with a 458 nm Argon laser line and detected between 463 and 485 nm; GFP was excited with a 488 nm Argon laser line and detected between 500 and 550 nm; mCitrine was excited with a 514 nm Argon laser line and detected between 525 and 550 nm; mCherry was excited with a 561 nm DPSS diode laser and detected between 570 and 620 nm. Highly fluorescent samples were imaged with a photomultiplier (PMT), whereas samples with low fluorescence were analyzed with HyDs (both Leica). For simultaneous imaging of multiple fluorophores, the sequential scan mode "between lines" was used. A line average of three was used for all scans. All images were captured as Z-stacks of single XY-optical sections with the Z-step size of each experiment indicated in figure legends. Image analysis was performed with Leica LAS X V3.5.1 (Leica). λ-scanning was performed by selecting an area of interest that was in focus and exhibited strong fluorescence. For measurements, the Leica TCS SP5 was run in xyλ-mode and the fluorescence emission was detected in 5 nm bins in a range of 500-760 nm (GFP) or 525-760 nm (mCitrine) using HyDs. Fluorophores were excited with a 488 nm (GFP) or 514 nm (mCitrine) Argon laser line. After scanning,  $\lambda$  emission

spectra were analyzed in selected regions-of-interest using Leica LAS X V3.5.1 (Leica). Results were exported as normalized mean fluorescence intensities and plotted in GraphPad Prism V8.0 (GraphPad Software, San Diego, CA, USA).

#### **FRET-FLIM** measurements

FRET-FLIM measurements were performed with an FCS/FLIM-FRET/rapidFLIM upgrade kit (Picoquant, Berlin, Germany) used in tandem with an Olympus (Tokyo, Japan) FV3000 mounted on an IX63 stand. This method was adapted from (Weidtkamp-Peters & Stahl, 2017). Please see File S1 for a detailed description of the technique.

#### Yeast two-hybrid assay

The yeast two-hybrid assays were adapted from (Engelhardt et al., 2023). Please see File S1 for a detailed description of the cloning.

#### RT-qPCR

Gene expression of 909, PLC1, and SAC-like was measured using RT-qPCR in mock-treated or Bh-infected barley epidermal peels at the indicated timepoints. As a housekeeping gene, ubiquitinconjugating enzyme 2 (UBC2) was used for barley, while  $\beta$ -tubulin 2 (β-TUB2) was used for Bh (Schnepf et al., 2018). Please see File S1 for a detailed description of the method.

#### Production and purification of recombinant proteins

For in vitro lipid-binding assays, proteins were produced in E. coli (strain Rosetta 2). For that, chemically competent bacteria were transformed with pGEX- and pMAL-plasmids containing the constructs-of-interest (see molecular cloning). One colony per construct was taken to inoculate 30 ml 2YT (10 g/L yeast extract, 16 g/L tryptone, 5 g/L NaCl, 2 g/L D-glucose) starter culture that was grown overnight at 18°C in a shaker. The next day, 300 ml of fresh 2YT medium were inoculated with 3 ml of starter culture and grown at 37°C under constant shaking until an oD600nm of 0.6-0.8 was reached. Bacterial growth was stopped by a 30 min incubation on ice, after which protein expression was started through the addition of sopropyl β-D-1-thiogalactopyranoside (IPTG) (final concentration: 0.1 mm). After induction, cultures were incubated for 18-20 h at 18°C under constant shaking. All cultures were harvested in 50 ml aliquots via centrifugation at 3000 a and 4°C. Cell pellets were frozen in liquid N₂ and stored at -80°C until use. Cell pellets were resuspended in 3 ml extraction buffer and incubated on ice for 30-45 min with occasional mixing. The extraction buffer for MBP-tagged proteins was: 20 mm Tris-HCl pH 7.4, 200 mm NaCl, 1 mm EDTA, 1× SigmaFast protease inhibitor cocktail without EDTA (Sigma-Aldrich), 1 mm DTT, 2 mg/ml lysozyme. For GST-tagged proteins, the extraction buffer was 50 mm Tris-HCl pH 7.4, 150 mm NaCl, 1x SigmaFast protease inhibitor cocktail without EDTA (Sigma-Aldrich), 1 mm DTT, 2 mg/ml lysozyme. After resuspension, cells were lysed through sonication, delivering 4000 J in 2 s pulses using a Vibra-Cell<sup>™</sup> 72 442 with Bransonic B12 Ultrasonics Sonifier (both from Branson Ultrasonics, Brookfield, WI, USA). Cell lysates were centrifuged at 20 000 g for 15 min at 4°C to separate supernatant and pellet fractions. The protein extracts in the supernatants were finally used for protein purification via affinity chromatography. MBP-fusion proteins were enriched via amylose resin (NEB, Ipswich, MA, USA), while GST-fusion proteins were enriched in Pierce™ glutathione agarose resin (Thermo Fisher Scientific). Both resins were packed into Pierce™ centrifugation columns (Thermo Fisher Scientific) before

#### 18 of 20 Lukas Sebastian Weiß et al.

use. To start, both columns were washed once with 3 ml  $ddH_2O$  and twice with either 3 ml MBP equilibration buffer (20 mm Tris–HCl pH 7.4, 200 mm NaCl, 1 mM EDTA, 1 mm DTT) or 3 ml GST equilibration buffer (50 mm Tris–HCl pH 7.4, 150 mm NaCl, 1 mm DTT). Between washing steps, columns were centrifuged for 1 min at 400  $\boldsymbol{g}$  and 4°C. Afterwards, raw protein extracts were added onto the columns and incubated for 1 h at room temperature in an overhead tumbler. Following that, each column was washed three times with its respective equilibration buffer from above. Lastly, fusion proteins were eluted in either MBP elution buffer (10 mm maltose, 20 mm Tris–HCl pH 7.4, 200 mm NaCl, 1 mm EDTA, 1 mm DTT) or GST elution buffer (50 mm glutathion, 50 mm Tris–HCl pH 7.4, 150 mm NaCl, 1 mm DTT). Proteins were stored at  $-80^{\circ}$ C until use.

#### Protein-lipid-overlay experiments

Commercially available membranes with pre-spotted lipids (PIP Strips, Echelon Biosciences Inc., MoBiTec GmbH, Göttingen, Germany) were first blocked with 3% (w/v) skimmed milk powder in TBS (50 mm Tris-HCl pH 7.5, 150 mm NaCl) for 30 min. Subsequently, membranes were incubated overnight with 0.5 µg/ml purified proteins in 3% skimmed milk in TBS at 4°C and gentle shaking. The next day, membranes were washed three times with TBS and incubated with primary antibodies in 3% skimmed milk in TBS for 1 h at room temperature with gentle shaking. Membranes were again washed three times with TBS before being incubated with secondary antibodies in 3% skimmed milk in TBS for 1 h at room temperature with gentle shaking. Afterwards, membranes were washed twice with TBS and once with AP-buffer (100 mm Tris-HCl pH 9.5, 100 mm NaCl, 5 mm MgCl<sub>2</sub>). Proteins were detected using 0.175 mg/ml BCIP (5-bromo-4-chloro-3-indolyl phosphate disodium salt; Roth, Karlsruhe, Germany) and 0.338 mg/ml NBT (nitro blue tetrazolium chloride; Roth) in AP-buffer. Reactions were stopped by washing with ddH2O when sufficient staining was attained. All antibodies can be found in Table S4.

#### **Bioinformatic analyses**

All bioinformatics analyses are described in File S1.

#### **AUTHOR CONTRIBUTIONS**

LSW and RH designed the study concept. All authors designed experiments. LSW, CB, MB, JM, MH, and GH performed the experiments. RH, BK, JK, JH, and SE supervised the work. RH, JK, JH, and BK provided resources. LSW and RH wrote the manuscript draft. All authors critically read and revised the manuscript and approved the final version.

# **ACKNOWLEDGMENTS**

We thank Yvon Jaillais (ENS Lyon) for providing the pB7m34GW-pUBQ10::Citrine-C2<sup>LACT</sup> plasmid and Masa Sato (Kyoto Prefectural University) for sending the pGWB501-UBQ10::mCitrine-2xML1N plasmid. We acknowledge Cornelia Marthe for technical assistance in generating the transgenic barley lines and thank Johanna Hofer and Vanessa Weiß for outstanding technical assistance in wet lab work at TU Munich. We thank Marina Hijano Moreno and Tina Reiner (TU Munich) for minor experimental contributions. We acknowledge the TUM Center for Advanced Light Microscopy (CALM) at the TUM School of Life Sciences Weihenstephan for providing their FRET-FLIM equipment and training and the TUM Plant Technology Center for support in the propagation of

transgenic barley seed. This study was supported by the German Research Foundation with grants within collaborative research centers SFB624 (grants to R.H. and B.K.) and HU886/12 (to R.H.). Open Access funding enabled and organized by Projekt DEAL.

#### **CONFLICT OF INTEREST**

The authors declare no conflict of interest.

#### **DATA AVAILABILITY STATEMENT**

The data that support the findings of this study are openly available in PRIDE at <a href="http://www.ebi.ac.uk/pride/archive/projects/PXD056811">http://www.ebi.ac.uk/pride/archive/projects/PXD056811</a>, reference number PXD056811.

#### SUPPORTING INFORMATION

Additional Supporting Information may be found in the online version of this article.

File S1. Additional Experimental Procedures and references.

Table S1. Full dataset from the barley eGFP-RACB-CA epidermis interactome.

Table S2. Primers.

Table S3. Genes.

Table S4. Antibodies.

Figure S1. RACB-CA epidermis interactome screening.

Figure S2. Annotation of functional domains and catalytic amino acids in PLC1 and SAC-like.

Figure S3. Homologs of 909, PLC1 and SAC-like in barley, rice, Arabidopsis, and Bh. Figure S1.

Figure S4. Zoom in magnification of phospholipid marker accumulation at sites of penetration by *B. hordei*.

Figure S5. Interaction of 909 with RACB in vivo and of 909, PLC1, and SAC-like with RACB in silico.

#### REFERENCES

- Akamatsu, A., Wong, H.L., Fujiwara, M., Okuda, J., Nishide, K., Uno, K. et al. (2013) An OsCEBiP/OsCERK1-OsRacGEF1-OsRac1 module is an essential early component of chitin-induced rice immunity. *Cell Host & Microbe*, 13, 465–476.
- Bak, G., Lee, E.J., Lee, Y., Kato, M., Segami, S., Sze, H. et al. (2013) Rapid structural changes and acidification of guard cell vacuoles during stomatal closure require phosphatidylinositol 3,5-bisphosphate. Plant Cell, 25, 2202–2216.
- Berken, A. (2006) ROPs in the spotlight of plant signal transduction. *Cellular and Molecular Life Sciences*, **63**, 2446–2459.
- Caldelari, D., Sternberg, H., Rodríguez-Concepción, M., Gruissem, W. & Yalovsky, S. (2001) Efficient prenylation by a plant Geranylgeranyltransferase-I requires a functional CaaL box motif and a proximal polybasic domain. Plant Physiology, 126, 1416–1429.
- Choi, S., Prokchorchik, M., Lee, H., Gupta, R., Lee, Y., Chung, E.H. et al. (2021) Direct acetylation of a conserved threonine of RIN4 by the bacterial effector HopZ5 or AvrBsT activates RPM1-dependent immunity in Arabidopsis. Molecular Plant, 14, 1951–1960.
- Choi, Y., Lee, Y., Kim, S.Y., Lee, Y. & Hwang, J.U. (2013) Arabidopsis ROP-interactive CRIB motif-containing protein 1 (RIC1) positively regulates auxin signalling and negatively regulates abscisic acid (ABA) signalling during root development. *Plant, Cell & Environment*, 36, 945–955.
- Cox, J. & Mann, M. (2008) MaxQuant enables high peptide identification rates, individualized ppb-range mass accuracies and proteome-wide protein quantification. *Nature Biotechnology*, 26, 1367–1372.
- Engelhardt, S., Trutzenberg, A., Kopischke, M., Probst, K., McCollum, C., Hofer, J. et al. (2023) Barley RIC157, a potential RACB scaffold protein, is involved in susceptibility to powdery mildew. Plant Molecular Biology, 111, 329–344.

- Frantzeskakis, L., Kracher, B., Kusch, S., Yoshikawa-Maekawa, M., Bauer, S., Pedersen, C. et al. (2018) Signatures of host specialization and a recent transposable element burst in the dynamic one-speed genome of the fungal barley powdery mildew pathogen. BMC Genomics, 19, 381.
- Fratini, M., Krishnamoorthy, P., Stenzel, I., Riechmann, M., Matzner, M., Bacia. K. et al. (2021) Plasma membrane nano-organization specifies phosphoinositide effects on rho-GTPases and actin dynamics in tobacco pollen tubes. Plant Cell, 33, 642-670.
- Fu, Y., Xu, T., Zhu, L., Wen, M. & Yang, Z. (2009) A ROP GTPase signaling pathway controls cortical microtubule ordering and cell expansion in Arabidopsis. Current Biology, 19, 1827-1832.
- Georges, F., Das, S., Ray, H., Bock, C., Nokhrina, K., Kolla, V.A. et al. (2009) Over-expression of Brassica napus phosphatidylinositol-phospholipase C2 in canola induces significant changes in gene expression and phytohormone distribution patterns, enhances drought tolerance and promotes early flowering and maturation. Plant, Cell & Environment, 32, 1664-1681.
- Gerth, K., Lin, F., Menzel, W., Krishnamoorthy, P., Stenzel, I., Heilmann, M. et al. (2017) Guilt by association: a phenotype-based view of the plant phosphoinositide network. Annual Review of Plant Biology, 68, 349-374.
- Gu, Y., Fu, Y., Dowd, P., Li, S., Vernoud, V., Gilroy, S. et al. (2005) A rho family GTPase controls actin dynamics and tip growth via two counteracting downstream pathways in pollen tubes. The Journal of Cell Biology, 169, 127-138.
- He, Q., Naqvi, S., McLellan, H., Boevink, P.C., Champouret, N., Hein, I. et al. (2018) Plant pathogen effector utilizes host susceptibility factor NRL1 to degrade the immune regulator SWAP70. Proceedings of the National Academy of Sciences of the United States of America, 115, E7834–E7843.
- Heo, W.D., Inoue, T., Park, W.S., Kim, M.L., Park, B.O., Wandless, T.J. et al. (2006) PI(3,4,5)P3 and PI(4,5)P2 lipids target proteins with polybasic clusters to the plasma membrane. Science, 314, 1458-1461.
- Hirano, T., Konno, H., Takeda, S., Dolan, L., Kato, M., Aoyama, T. et al. (2018) Ptdlns(3,5)P2 mediates root hair shank hardening in Arabidopsis. Nature Plants, 4, 888-897
- Hirano, T., Stecker, K., Munnik, T., Xu, H. & Sato, M.H. (2017) Visualization of phosphatidylinositol 3,5-bisphosphate dynamics by a tandem ML1Nbased fluorescent protein probe in Arabidopsis. Plant & Cell Physiology,
- Hoefle, C., Huesmann, C., Schultheiss, H., Bornke, F., Hensel, G., Kumlehn, J. et al. (2011) A barley ROP GTPase ACTIVATING PROTEIN associates with microtubules and regulates entry of the barley powdery mildew fungus into leaf epidermal cells. Plant Cell, 23, 2422-2439.
- Huesmann, C., Reiner, T., Hoefle, C., Preuss, J., Jurca, M.E., Domoki, M. et al. (2012) Barley ROP binding kinase1 is involved in microtubule organization and in basal penetration resistance to the barley powdery mildew fungus. Plant Physiology, 159, 311-320.
- Ischebeck, T., Stenzel, I., Hempel, F., Jin, X., Mosblech, A. & Heilmann, I. Phosphatidylinositol-4,5-bisphosphate influences mediated cell expansion in pollen tubes of Nicotiana tabacum. Plant Journal, 65, 453-468.
- Jezyk, M.R., Snyder, J.T., Gershberg, S., Worthylake, D.K., Harden, T.K. & Sondek, J. (2006) Crystal structure of Rac1 bound to its effector phospholipase C-beta2. Nature Structural & Molecular Biology, 13, 1135-1140.
- Jones, M.A., Shen, J.J., Fu, Y., Li, H., Yang, Z. & Grierson, C.S. (2002) The Arabidopsis Rop2 GTPase is a positive regulator of both root hair initiation and tip growth. Plant Cell, 14, 763-776.
- Kost, B. (2008) Spatial control of rho (Rac-Rop) signaling in tip-growing plant cells. Trends in Cell Biology, 18, 119-127.
- Kost, B., Lemichez, E., Spielhofer, P., Hong, Y., Tolias, K., Carpenter, C. et al. (1999) Rac homologues and compartmentalized phosphatidylinositol 4, 5-bisphosphate act in a common pathway to regulate polar pollen tube growth. Journal of Cell Biology, 145, 317-330.
- Kulich, I., Vogler, F., Bleckmann, A., Cyprys, P., Lindemeier, M., Fuchs, I. et al. (2020) ARMADILLO REPEAT ONLY proteins confine rho GTPase signalling to polar growth sites. Nature Plants, 6, 1275-1288.
- Kusano, H., Testerink, C., Vermeer, J.E., Tsuge, T., Shimada, H., Oka, A. et al. (2008) The Arabidopsis phosphatidylinositol phosphate 5-kinase PIP5K3 is a key regulator of root hair tip growth. Plant Cell, 20, 367-380.
- Kwaaitaal, M., Nielsen, M.E., Bohlenius, H. & Thordal-Christensen, H. (2017) The plant membrane surrounding powdery mildew haustoria shares

- properties with the endoplasmic reticulum membrane. Journal of Experimental Botany, 68, 5731-5743.
- Lavy, M., Bloch, D., Hazak, O., Gutman, I., Poraty, L., Sorek, N. et al. (2007) A novel ROP/RAC effector links cell polarity, root-meristem maintenance, and vesicle trafficking. Current Biology, 17, 947-952.
- Lavy, M. & Yalovsky, S. (2006) Association of Arabidopsis type-II ROPs with the plasma membrane requires a conserved C-terminal sequence motif and a proximal polybasic domain. Plant Journal, 46, 934-947.
- Lazo, G.R., Stein, P.A. & Ludwig, R.A. (1991) A DNA transformationcompetent Arabidopsis genomic library in agrobacterium. Bio/Technoloav. 9. 963-967.
- Li, S., Gu, Y., Yan, A., Lord, E. & Yang, Z.B. (2008) RIP1 (ROP interactive partner 1)/ICR1 marks pollen germination sites and may act in the ROP1 pathway in the control of polarized pollen growth. Molecular Plant, 1, 1021-1035
- Li, S., Wang, Q., Wang, Y., Chen, X. & Wang, Z. (2009) PLC-gamma1 and Rac1 coregulate EGF-induced cytoskeleton remodeling and cell migration. Molecular Endocrinology, 23, 901-913.
- Liao, W., Nielsen, M.E., Pedersen, C., Xie, W. & Thordal-Christensen, H. (2023) Barley endosomal MONENSIN SENSITIVITY1 is a target of the powdery mildew effector CSEP0162 and plays a role in plant immunity. Journal of Experimental Botany, **74**, 118–129.
- Lin, D., Cao, L., Zhou, Z., Zhu, L., Ehrhardt, D., Yang, Z. et al. (2013) Rho GTPase signaling activates microtubule severing to promote microtubule ordering in Arabidopsis. Current Biology, 23, 290-297.
- Liu, H.-T., Huang, W.-D., Pan, Q.-H., Weng, F.-H., Zhan, J.-C., Liu, Y. et al. (2006) Contributions of PIP2-specific-phospholipase C and free salicylic acid to heat acclimation-induced thermotolerance in pea leaves. Journal of Plant Physiology, 163, 405-416.
- Lück, S., Kreszies, T., Strickert, M., Schweizer, P., Kuhlmann, M. & Douchkov, D. (2019) siRNA-finder (si-fi) software for RNAi-target design and off-target prediction. Frontiers in Plant Science, 10, 1023.
- Mackey, D., Holt, B.F., III, Wiig, A. & Dangl, J.L. (2002) RIN4 interacts with pseudomonas syringae type III effector molecules and is required for RPM1-mediated resistance in Arabidopsis. Cell. 108, 743-754.
- Mao, Y. & Tan, S. (2021) Functions and mechanisms of SAC phosphoinositide phosphatases in plants. Frontiers in Plant Science, 12, 803635.
- Mascher, M., Gundlach, H., Himmelbach, A., Beier, S., Twardziok, S.O. Wicker, T. et al. (2017) A chromosome conformation capture ordered sequence of the barley genome. Nature, 544, 427-433.
- McCollum, C., Engelhardt, S., Weiss, L. & Huckelhoven, R. (2020) ROP INTERACTIVE PARTNER b interacts with RACB and supports fungal penetration into barley epidermal cells. Plant Physiology, 184, 823-836.
- Menzel, W., Stenzel, I., Helbig, L.M., Krishnamoorthy, P., Neumann, S., Eschen-Lippold, L. et al. (2019) A PAMP-triggered MAPK cascade inhibits phosphatidylinositol 4,5-bisphosphate production by PIP5K6 in Arabidopsis thaliana. The New Phytologist, 224, 833-847.
- Mueller-Roeber, B. & Pical, C. (2002) Inositol phospholipid metabolism in Arabidopsis. Characterized and putative isoforms of inositol phospholipid kinase and phosphoinositide-specific phospholipase C. Plant Physiology, 130, 22-46.
- Nielsen, M.E. (2024) Vesicle trafficking pathways in defence-related cell wall modifications: papillae and encasements. Journal of Experimental Botany, 75, 3700-3712.
- Noack, L.C. & Jaillais, Y. (2020) Functions of anionic lipids in plants. Annual Review of Plant Biology, 71, 71-102.
- Nottensteiner, M., Zechmann, B., McCollum, C. & Huckelhoven, R. (2018) A barley powdery mildew fungus non-autonomous retrotransposon encodes a peptide that supports penetration success on barley. Journal of Experimental Botany, 69, 3745-3758.
- Nováková, P., Hirsch, S., Feraru, E., Tejos, R., van Wijk, R., Viaene, T. et al. (2014) SAC phosphoinositide phosphatases at the tonoplast mediate vacuolar function in Arabidopsis. Proceedings of the National Academy of Sciences of the United States of America, 111, 2818-2823.
- Pedersen, C., van Themaat, E.V.L., McGuffin, L., Abbott, J., Burgis, T., Barton, G. et al. (2012) Structure and evolution of barley powdery mildew effector candidates, BMC Genomics, 13, 694.
- Platre, M.P., Bayle, V., Armengot, L., Bareille, J., Marquès-Bueno, M.d.M., Creff, A. et al. (2019) Developmental control of plant rho GTPase nanoorganization by the lipid phosphatidylserine. Science, 364, 57-62.

- Platre, M.P., Noack, L.C., Doumane, M., Bayle, V., Simon, M.L.A., Maneta-Peyret, L. et al. (2018) A combinatorial lipid code shapes the electrostatic landscape of plant Endomembranes, Developmental Cell. 45, 465-480.
- Pokotylo, I., Kolesnikov, Y., Kravets, V., Zachowski, A. & Ruelland, E. (2014) Plant phosphoinositide-dependent phospholipases C: variations around a canonical theme. Biochimie. 96, 144-157.
- Qin, L., Zhou, Z., Li, Q., Zhai, C., Liu, L., Quilichini, T.D. et al. (2020) Specific recruitment of phosphoinositide species to the plant-pathogen interfacial membrane underlies Arabidopsis susceptibility to fungal infection. Plant Cell. 32, 1665-1688.
- Rao, J.N., Liu, S.V., Zou, T., Liu, L., Xiao, L., Zhang, X. et al. (2008) Rac1 promotes intestinal epithelial restitution by increasing Ca2+ influx through interaction with phospholipase C-(gamma)1 after wounding. American Journal of Physiology-Cell Physiology, 295, C1499-C1509.
- Rapazote-Flores, P., Bayer, M., Milne, L., Mayer, C.D., Fuller, J., Guo, W. et al. (2019) BaRTv1.0: an improved barley reference transcript dataset to determine accurate changes in the barley transcriptome using RNA-seq. BMC Genomics, 20, 968.
- Rausche, J., Stenzel, I., Stauder, R., Fratini, M., Trujillo, M., Heilmann, I. et al. (2021) A phosphoinositide 5-phosphatase from Solanum tuberosum is activated by PAMP-treatment and may antagonize phosphatidylinositol 4,5-bisphosphate at Phytophthora infestans infection sites. The New Phytologist, 229, 469-487.
- Reiner, T., Hoefle, C. & Huckelhoven, R. (2016) A barley SKP1-like protein controls abundance of the susceptibility factor RACB and influences the interaction of barley with the barley powdery mildew fungus. Molecular Plant Pathology, 17, 184-195.
- Sabelleck, B., Deb, S., Levecque, S.C.J., Freh, M., Reinstädler, A., Spanu, P.D. et al. (2025) A powdery mildew core effector protein targets the host endosome tethering complexes HOPS and CORVET in barley. Plant Phys-
- Saur, I.M.L. & Hückelhoven, R. (2021) Recognition and defence of plantinfecting fungal pathogens. Journal of Plant Physiology, 256, 153324.
- Schmelzer, E. (2002) Cell polarization, a crucial process in fungal defence. Trends in Plant Science, 7, 411-415.
- Schnepf, V., Vlot, A.C., Kugler, K. & Hückelhoven, R. (2018) Barley susceptibility factor RACB modulates transcript levels of signalling protein genes in compatible interaction with Blumeria graminis f.sp. hordei. Molecular Plant Pathology, 19, 393-404.
- Schultheiss, H., Dechert, C., Kogel, K.H. & Huckelhoven, R. (2002) A small GTP-binding host protein is required for entry of powdery mildew fungus into epidermal cells of barley. Plant Physiology, 128, 1447-1454.
- Schultheiss, H., Dechert, C., Kogel, K.H. & Huckelhoven, R. (2003) Functional analysis of barley RAC/ROP G-protein family members in susceptibility to the powdery mildew fungus. The Plant Journal, 36, 589-601.
- Schultheiss, H., Preuss, J., Pircher, T., Eichmann, R. & Huckelhoven, R. (2008) Barley BIC171 interacts with BACB in planta and supports entry of the powdery mildew fungus. Cellular Microbiology, 10, 1815-1826.
- Schweizer, P., Christoffel, A. & Dudler, R. (1999) Transient expression of members of the germin-like gene family in epidermal cells of wheat confers disease resistance. The Plant Journal, 20, 541-552.
- Sherwood, J.E. & Somerville, S.C. (1990) Sequence of the Erysiphe graminis f. sp. hordei gene encoding beta-tubulin. Nucleic Acids Research, 18,
- Shimada, T.L., Betsuyaku, S., Inada, N., Ebine, K., Fujimoto, M., Uemura, T. et al. (2019) Enrichment of phosphatidylinositol 4,5-bisphosphate in the extra-invasive hyphal membrane promotes Colletotrichum infection of Arabidopsis thaliana. Plant & Cell Physiology, 60, 1514-1524.
- Simon, M.L., Platre, M.P., Assil, S., van Wijk, R., Chen, W.Y., Chory, J. et al. (2014) A multi-colour/multi-affinity marker set to visualize phosphoinositide dynamics in Arabidopsis. Plant Journal, 77, 322-337.
- Song, F. & Goodman, R.M. (2002) Molecular cloning and characterization of a rice phosphoinositide-specific phospholipase C gene, OsPI-PLC1, that is activated in systemic acquired resistance. Physiological and Molecular Plant Pathology, 61, 31-40.

- Sorek, N., Poraty, L., Sternberg, H., Buriakovsky, E., Bar, E., Lewinsohn, E. et al. (2017) Corrected and republished from: activation status-coupled transient S-acylation determines membrane partitioning of a plant rhorelated GTPase. Molecular and Cellular Biology, 37, e00333-17
- Spanu, P.D., Abbott, J.C., Amselem, J., Burgis, T.A., Soanes, D.M., Stuber, K. et al. (2010) Genome expansion and gene loss in powdery mildew fungi reveal tradeoffs in extreme parasitism. Science, 330, 1543-1546.
- Stanislas, T., Huser, A., Barbosa, I.C., Kiefer, C.S., Brackmann, K., Pietra, S. et al. (2015) Arabidopsis D6PK is a lipid domain-dependent mediator of root epidermal planar polarity. Nature Plants, 1, 15162.
- Sternberg, H., Buriakovsky, E., Bloch, D., Gutman, O., Henis, Y.I. & Yalovsky, S. (2021) Formation of self-organizing functionally distinct rho of plants domains involves a reduced mobile population. Plant Physiology, 187, 2485-2508.
- Tripathy, M.K., Tyagi, W., Goswami, M., Kaul, T., Singla-Pareek, S.L., Deswal, R. et al. (2011) Characterization and functional validation of tobacco PLC Delta for abiotic stress tolerance. Plant Molecular Biology Reporter, 30 488-497
- Trutzenberg, A., Engelhardt, S., Weiß, L. & Hückelhoven, R. (2022) Barley guanine nucleotide exchange factor Hv GEF14 is an activator of the susceptibility factor Hv RACB and supports host cell entry by Blumeria graminis f. sp. hordei. Molecular Plant Pathology, 23, 1524-1537.
- Tyanova, S., Temu, T., Sinitcyn, P., Carlson, A., Hein, M.Y., Geiger, T. et al. (2016) The Perseus computational platform for comprehensive analysis of (prote) omics data. Nature Methods, 13, 731-740.
- van Leeuwen, W., Vermeer, J.E., Gadella, T.W., Jr. & Munnik, T. (2007) Visualization of phosphatidylinositol 4,5-bisphosphate in the plasma membrane of suspension-cultured tobacco BY-2 cells and whole Arabidopsis seedlings. Plant Journal, 52, 1014-1026.
- van Schie, C.C. & Takken, F.L. (2014) Susceptibility genes 101: how to be a good host. Annual Review of Phytopathology, 52, 551-581.
- Vossen, J.H., Abd-El-Haliem, A., Fradin, E.F., van den Berg, G.C., Ekengren, S.K., Meijer, H.J. et al. (2010) Identification of tomato phosphatidylinositol-specific phospholipase-C (PI-PLC) family members and the role of PLC4 and PLC6 in HR and disease resistance. Plant Journal. 62, 224-239.
- Wang, C.R., Yang, A.F., Yue, G.D., Gao, Q., Yin, H.Y. & Zhang, J.R. (2008) Enhanced expression of phospholipase C 1 (ZmPLC1) improves drought tolerance in transgenic maize. Planta, 227, 1127-1140.
- Weidtkamp-Peters, S. & Stahl, Y. (2017) The use of FRET/FLIM to study proteins interacting with plant receptor kinases. In: Aalen, R.B. (Ed.) Plant receptor kinases: methods and protocols. New York, NY: Springer New
- Weiss, L., Gaelings, L., Reiner, T., Mergner, J., Kuster, B., Feher, A. et al. (2022) Posttranslational modification of the RHO of plants protein RACB by phosphorylation and cross-kingdom conserved ubiquitination. PLoS One. 17, e0258924.
- Winge, P., Brembu, T., Kristensen, R. & Bones, A.M. (2000) Genetic structure and evolution of RAC-GTPases in Arabidopsis thaliana. Genetics, 156,
- Wu, G., Gu, Y., Li, S. & Yang, Z. (2001) A genome-wide analysis of Arabidopsis Rop-interactive CRIB motif-containing proteins that act as Rop GTPase targets. The Plant Cell. 13, 2841-2856.
- Yalovsky, S. (2015) Protein lipid modifications and the regulation of ROP GTPase function. Journal of Experimental Botany, 66, 1617-1624.
- Yang, Y., Li, R. & Qi, M. (2000) In vivo analysis of plant promoters and transcription factors by agroinfiltration of tobacco leaves. The Plant Journal, 22. 543-551.
- Yang, Z. (2002) Small GTPases: versatile signaling switches in plants. Plant Cell, 14(Suppl), S375-S388.
- Zhong, R. & Ye, Z.H. (2003) The SAC domain-containing protein gene family in Arabidopsis. Plant Physiology, 132, 544-555.
- Zhou, Z., Shi, H., Chen, B., Zhang, R., Huang, S. & Fu, Y. (2015) Arabidopsis RIC1 severs actin filaments at the apex to regulate pollen tube growth. The Plant Cell, 27, 1140-1161.